DEVELOPMENT AND LAB CALIBRATION OF THE PNEUMATIC IN-SITU SOIL CAVING INDEX SAMPLER (PISCIS)

A Thesis

presented to

the Faculty of California Polytechnic State University,

San Luis Obispo

In Partial Fulfillment

of the Requirements for the Degree

Master of Science in Civil and Environmental Engineering

by

Michael A. Grolle

March 2015

COMMITTEE MEMBERSHIP

TITLE:	Development And Lab Calibration of the Pneumatic In-situ Soil Caving Index Sampler (PISCIS)
AUTHOR:	Michael A. Grolle
DATE SUBMITTED:	March 2015
COMMITTEE CHAIR:	Robb Moss, Ph.D. Associate Professor of Civil Engineering
COMMITTEE MEMBER:	Gregg Fiegel, Ph.D. Professor of Civil Engineering
COMMITTEE MEMBER:	James Hanson, Ph.D. Professor of Civil Engineering
COMMITTEE MEMBER:	Rob Down Lecturer of Architectural Engineering

ABSTRACT

Development And Lab Calibration of the Pneumatic In-situ Soil Caving Index Sampler (PISCIS)

Michael A. Grolle

The caving/sloughing of sandy layers into drilled shafts is a common and costly phenomenon in the drilling industry. A prototype soil-testing device known as the Pneumatic In-situ Soil Caving Index Sampler (PISCIS) has been developed to test sandy layers above the water table for their propensity to cave/slough into a drilled shaft during the drilling process. The PISCIS fits down a Cone Penetration Test (CPT) hole and uses air pressure to agitate a sample off of the hole wall that is then collected and weighed. Large-scale lab testing was conducted using sand under a variety of simulated overburden pressures and fines contents. The tests were conducted with a dual purpose in mind. First, the tests confirmed the functionality of the PISCIS prototype and its ability to collect samples in a consistent and repeatable manner. Second, the tests resulted in a calibration curve that shows a very strong (nearly exponential) relationship between collected sample weight and the fines content of the test sand; higher fines contents resulted in lower collection weights. The PISCIS was designed to supplement information found in a geotechnical report with information that would specifically inform drilling contractors about potential caving/ sloughing hazards found in the stratigraphy.

ACKNOWLEDGMENTS

This thesis is dedicated to my parents, Dr. and Mrs. Kenneth F. Grolle. For 30 years they have raised, supported, and encouraged me, and have always led by example. They have been the source of mental fortitude that has made my achievements possible both in life, and in academics.

I would like to thank my loving wife, Kerry S. Grolle, for her unwavering support, encouragement, and optimism. Without her, I never would have taken on such a massive endeavor, let alone felt I could complete the task. My father and mother-in-law, Mr. and Mrs. Leslie D. Scott, have also been a vast source of knowledge and support throughout the entire process.

I would like to thank my professor and graduate advisor, Dr. Robb Moss, for his guidance, enthusiasm, and criticism throughout my research, as well as in the classroom. His research experience, and willingness to share his knowledge, proved to be invaluable when faced with overwhelming amounts of possibilities and directions.

I would like to express my gratitude to my committee members for their time and effort in participating in, and providing critical analysis of my work; Professor Rob Down, Dr. James Hanson, Dr. Gregg Fiegel, and Dr. Robb Moss.

Additional support was provided through donations of time and materials from Paso Robles Tank Inc., Case Pacific Co., and Lesco Engines. I would like to extend thanks to these local businesses for their generosity in furthering student research.

TABLE OF CONTENTS

LIST OF FIGURES

CHAPTER 1: STATEMENT OF RESEARCH

1.1 Introduction

Drilled shafts are a common foundation type in many large building and infrastructure projects. They are used primarily as foundation elements that can reach through less competent soils down to bedrock or stronger soil that can support the expected structural loads. The construction of such foundations is typically the responsibility of a specialized drilling contractor. Drilling contractors rely entirely on local experience in tandem with the information provided in the geotechnical report to predict drilling conditions and ultimately the cost of drilling.

Drilling contractors pay particular attention to any layers of sand shown in the subsurface profile, as these layers can be problematic. If the sand layer is classified as 'loose' or 'very loose' per ASTM D1586 and the percent passing a #200 sieve is less than 15% by weight, the sand may be susceptible to caving during the drilling process. Caving is a phenomenon that occurs when large volumes of soil slough off of the walls and fall into the shaft opening; this results in a large bell shaped void in the shaft or even an instability in the ground surface. Both of the aforementioned side effects of caving can result in expensive and unforeseen costs to a project and, specifically, the drilling contractor. Therefore, drilling contractors do not drill through layers of loose sand using the same procedure as drilling in dense sand.

Caving can be prevented with the use of either a steel casing that is advanced into the ground at the same time the hole is being excavated, or with the use of drilling slurry which applies a pressure to the walls of the hole in order to provide stability. These methods (casing and slurry drilling) involve more equipment, more sophisticated machinery, and tend to take up to twice as long to complete a shaft. This translates directly to a higher cost to both the client and the contractor (approximately two-fold). Because of this significant difference in equipment and cost, contractors will rarely take the risk of assuming the sand layer will not cave, but would rather bid the project as though the sand will cave as to avoid unforeseen costs regardless of how the sand behaves while drilling.

If additional information regarding suspect sand layers (loose with low percent fines content) were provided in the geotechnical report, contractors could more accurately identify drilling hazards and adjust their budgets accordingly allowing all parties involved to save time, energy, and money.

1.2 Project Scope

Depending on the project budget, a variety of tests can be conducted and reported, but nearly every soils report will contain data gathered from a Standard Penetration Test (SPT) rig. Using the SPT, a rough stratigraphy can be postulated, the density of soil layers can be estimated, and physical samples can be extracted for further lab testing. Layers of loose sand are identified as well as the percentage by weight of fines the sand contains.

Projects that have higher budgeting allotments to planning and site investigation, or more critical functions, will also hire a Cone Penetration Test (CPT) rig to gather more detailed and continuous soil data. The cone penetrometer is a calibrated sensor located at the end of a series of steel rods that can measure penetration resistance, frictional resistance, and pore pressure as it is advanced into the ground via a hydraulic jack. The CPT rig can reasonably locate and define a layer of loose sand as the cone is passing through it. Upon completing a cone penetration test, the sensor and steel rods are extracted from the ground, leaving a small hole where the rods once were.

If a test device were developed that could be lowered into a recently vacated test hole (left by the cone penetrometer) down to a level where the CPT sounding had identified a layer of loose sand, it may be possible to directly test that layer for its propensity to cave during drilling. This test device provides additional information that would allow contractors to adjust their bids and budgets appropriately for each site condition. It is the overlying and long-term goal of this thesis research to create such a device. The scope of this project begins with research and design and ends with the lab calibration of a functioning prototype. This prototype is called the Pneumatic In-situ Soil Caving Index Sampler, or PISCIS.

1.3 Organization of Thesis

Chapter 2 of this thesis summarizes the reviewed literature and explains the industry related merit in conducting this research. Chapter 3 details the experimental and laboratory test design used to conduct the research and collect data. Chapter 3 also contains the design and results of lab tests that preceded PISCIS testing. Chapter 4 briefly describes the prototype evolution and the design of the Pneumatic In-situ Soil Caving Index Sampler. Chapter 5 presents the results of the laboratory testing and discusses the significance of these results. Finally, Chapter 6 draws conclusions and suggests directions for future research and prototype development.

CHAPTER 2: LITERATURE REVIEW AND INDUSTRY RESEARCH

2.1 Literature Review

2.1.1 Effective Shear Strength and Caving

The effective shear strength of soil is directly responsible for the ability of the soil to resist the stresses that lead to caving/sloughing in an open borehole. The effective shear strength of soils is a complex property that varies greatly from one soil to the next. Defined generally, effective shear strength is comprised of two independent constituent strengths: frictional strength derived from particle contacts and soil fabric, and cohesive strength from interparticle physicochemical forces. Loose and very loose sands and silty sands are of particular interest in this research because, of all known soil types, these are the most likely to cave in an open borehole; This is because, as soil density decreases to the "loose" or "very loose" state (0-35% relative density), particle interlocking and contact friction reduces, thus decreasing shear strength. Additionally, the non-cohesive nature of sand and silts significantly reduce the cohesive strength component of effective shear strength.

Less generally speaking, the effective shear strength of sands and silty sands is dependent on many specific soil characteristics and soil states. Understanding these characteristics and their effects on shear strength will further assist in understanding what influences caving in sand layers. Charkraborty and Salgado (2010) studied the effects of confining pressure and dilatancy as it relates to effective shear strength in clean sand. They conclude that sand dilates more with increasing relative density and decreasing confinement. As dilatancy increases, the peak angle of internal friction increases, thereby increasing effective shear strength. Igwe et al. (2012) elaborated on this topic by experimenting on sands with variable gradation and densities. Their research shows that, while medium dense to dense specimens exhibit dilatant behavior, loose and very loose specimens behave contractively across all gradations tested. Narrowly-graded, gap-graded, and intermediately graded specimens have lower undrained peak shear strengths than well-graded specimens. The study also concluded that undrained residual shear strength is independent of normal stress for a given relative density. Belkhatir et al. (2013) studied the undrained shear strength of sand as the fines content increased with the addition of low-plasticity silt. They found that

increasing fines content reduces the undrained peak shear strength of the mixture. Their research also supports the concept of increasing shear strength with increasing relative density for a given fines content. A study by Salgado et al. (2000) evaluated the shear strength and stiffness of a range of sand and low plasticity fines combinations under drained conditions. They concluded that, as fines content increases to a threshold of 20%, the small strain shear modulus (G_o) decreases, but as the shearing progressed to larger strains, the addition of fines increased particle interlocking, dilatancy, and peak shear strength of the mixtures above that of clean sand. It was noted that the results of this study are "…strictly applicable only to the silt and sand gradations used in the testing" and that further study is required to assess these trends for different gradations of silty sand. Their conclusions about increasing peak shear strength with the addition of fines do not necessarily conflict with the study by Belkhatir et al. because one study was conducted in an undrained condition while the other was in a drained condition.

The disparity in the conclusions from the two aforementioned studies emphasizes the importance of moisture content and pore pressures on the effective shear strength of sand and silt mixtures. A study by Lu et al. (2007) examines the tensile strength of unsaturated sands, which is synonymous with the cohesive term of effective shear strength. The study examined tensile strengths of three different sand gradations both theoretically and experimentally, one of which was a silty sand. The theoretical results indicate that tensile stress present in sands, due to the presence of water in the void space, is inversely proportional to the particle diameter of the grains. The experimental results agree with the theoretical prediction of tensile strength, reaching a maximum of 1,448 pascals in the silty sand compared to 667 pascals in fine sand. This strength is generally due to the adhesion of water to sand particles and the formation of water bridges spanning between adjacent particles as well as negative pore pressures. The smaller the void space between particles, the more readily these bridges can form. Ning et al. discussed the tensile strength of unsaturated sand as it relates to three different water retention regimes: pendular, funicular, and capillary. The different regimes represent the spectrum of water contents over which the behavior of the water on and around soil particles behaves differently. The tensile strength of the soil due to the behavior of water increases with increasing water content in the pendular

regime and into the funicular regime, where strength peaks. After the peak, the strength decreases with increasing water content into the capillary regime. The water contents that define the boundaries between the various regimes vary greatly from one soil to the next depending on particle packing order and soil fabric.

2.1.2 The Mechanics of Caving in Drilled Shafts

Caving and sloughing of soils is a common hazard in the drilling industry, especially in loose sand. Extensive research (fueled primarily by the petroleum industry) has been conducted to define and predict caving of loose soil into boreholes. Wang and Sterling (2007) analyzed the stability of boreholes using a finite element analysis for horizontally drilled shafts. They concluded that there is an optimal drilling fluid pressure to maintain borehole stability in loose sands (initial static earth pressure), but too much pressure can lead to failures known as hydraulic fracturing. Other research presented by Chao et al. in 2008 uses seismic properties and soil attributes from loggings as inputs into a adaptive computer model to predict the proper drilling fluid density to maintain borehole stability in real-time. Bell (2003) outlined the use of down-hole imaging in conjunction with boring logs, known geologic formations, and exposed fractures to macroscopically map a large area in order to predict the stability of future boreholes when drilling in sedimentary rock. Research by Sanchez and Al-Harthy (2011) discussed the benefits of well planned drilling while simultaneously casing the hole to preemptively mitigate borehole instability hazards; this method is known as Casing-while-Drilling or CwD. As seen above, there exists a great deal of literature focused on predicting and mitigating drilling hazards in rock or in soil with the use of drilling fluid, but no literature encountered that discusses caving/sloughing in sands above the water table in an auger-drilled open borehole.

Although no extant literature specifically addresses the mechanics of caving in unsupported drilled shafts, research has been conducted to define horizontal earth pressure in sand, which is closely related to caving failures. Tobar and Meguid (2010) presented a comparison of various theoretical and experimental methods of determining earth pressures on cylindrical shafts in cohesionless material; These methods differ in their conclusions about the wall movements required for the active earth pressure condition to be achieved, but all agree

that earth pressures are reduced with increasing wall movements due to the soil mass moving toward a plastic equilibrium. The experimental model by Tobar and Meguid used a cylindrical device, outfitted with external load cells, that could contract radially to measure the response of the surrounding sand. This model most closely simulates the excavation of a shaft in loose sand, but does not account for the progression of the excavation downward in stages. Tobar and Meguid conclude that further research is required for shafts whose depth exceeds the diameter due to the solutions becoming "..more sensitive to the ratio between the vertical and horizontal arching".

A connection can be drawn between the failure of vertical cut slopes and the mechanisms that cause caving in drilled shafts. The similarity is particularly evident when looking at the Rankine earth-pressure model discussed in Tobar and Meguid. When looking at both a vertical cut slope and a drilled shaft in section (see Figure 2.1) the similarities become more graphically apparent. The overburden pressure of overlying soils in a drilled shaft is analogous to a surcharge load distributed above a vertical cut slope. When making a vertical cut in soil, the effective shear strength of the soil is primarily responsible for the ability of the soil to stand. Cohesionless soil, by definition, cannot stand in a vertical cut even though this happens frequently (albeit, temporarily) in practice due to capillary tension, mineral cementation, or particle interlocking due to the effects of aging. It is the cohesive term in the effective shear strength equation ($\tau = \sigma_n' \tan \phi' + \mathbf{c}$) that plays the major role in the stability of vertical cuts. Granular soils, in general, rely on the presence of smaller particles and water to provide this cohesion; therefore, again speaking generally, the more clay or silt present in sand, the more resistant a vertical cut in that soil would be to slope failures. The same can be said for granular soils encountered while drilling an unsupported vertical shaft.

If a granular soil is insufficiently cohesive, a series of progressive shear failures occur that cause the soil to slough off of the hole walls as the shaft is excavated downwards. This shear failure, known in the drilling industry as caving, occurs until the sand layer reaches a state of static or plastic equilibrium and, depending on the thickness of the layer being drilled through, can result in a large void within the drilled shaft. An image of one such void can be seen in Figure 2.2. One principle difference between caving in shafts and failures of cut slopes pertains to how the boundary conditions affect the propagation of shear failure surfaces

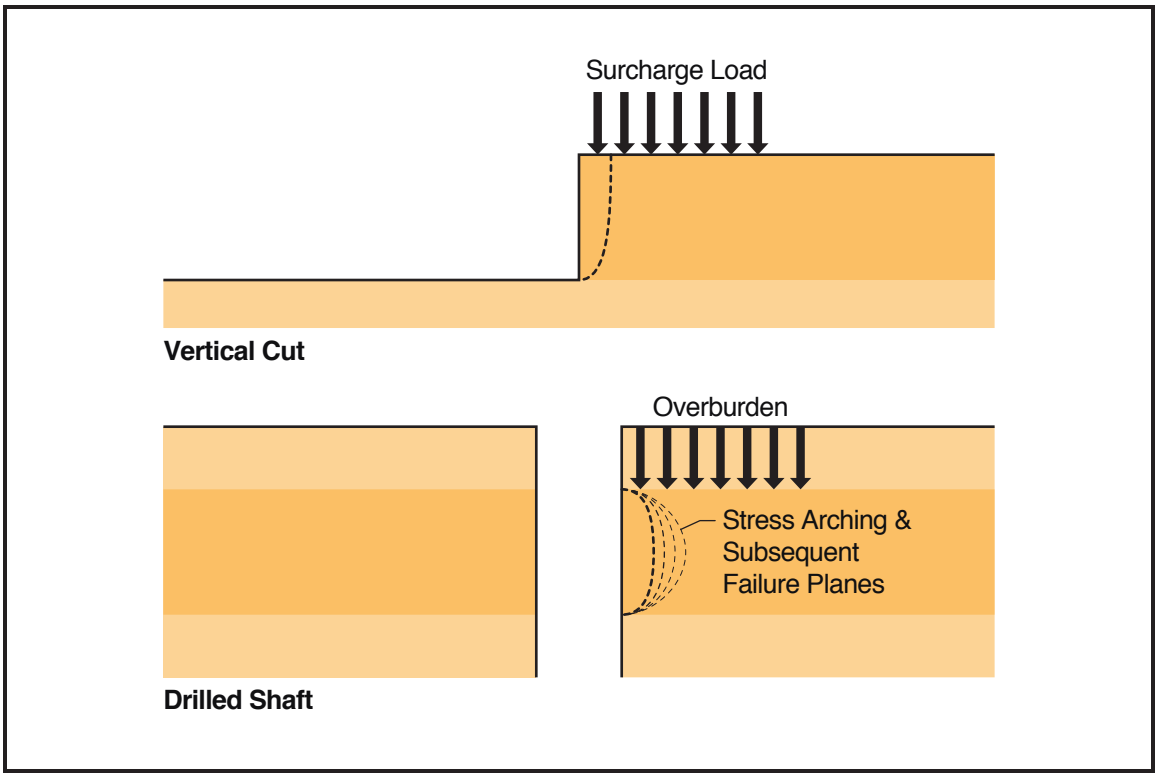

FIGURE 2.1: Comparison of Cut Slopes and Drilled Shafts

through the soil. In a vertical cut slope, the ground surface is free to move as a critical shear surface forms and the slope fails. This is not the case for drilled shafts. In a drilled shaft, the upper surface of an unstable layer is partially restricted from free movement by the overlying layer of soil; this generates a complex stress bridging scenario in which the overburden stress arches from one stable layer to the next through the less stable layer while still allowing a series of shear failures to occur. Subsequent failures force the stress path to deviate further from vertical and begin to concentrate the stress on and behind the newly exposed hole wall surfaces (see dotted shear failure surfaces in Figure 2.1). Stress concentrations will increase the shear strength of granular soil until static or plastic equilibrium is reached or a larger failure occurs in the surrounding soil. The extent of these failures is highly dependant on the properties of the less stable soil layer (i.e. density, grain size distribution, fines content, type of fines, moisture content, internal angle of friction, particle shape, void ratio, and so on). Although most of these properties can be collected through in-situ field tests, the behavior of granular soils during drilling "…cannot be predicted unless there is prior experience with the specific formation being excavated or full-sized test excavations have been made

during site characterization." (Brown, 2010). This claim is supported by the conclusions of research conducted by Tobar et al. (2010), Kim et al. (2013), and Pardo and Saez (2014) on the aforementioned arching effect that suggest that higher confining pressures in deep excavations increase the effects of arching and that further research is required to understand how this phenomenon affects the earth pressures in deep excavations. The results of stability analyses in drilled shaft excavations are unreliable when the vertical and horizontal earth pressures cannot be accurately defined.

FIGURE 2.2: Down Hole View of Shaft Caving

2.1.3 Drilling Stresses and Caving in Practice

Although there is extensive research in the drilling industry for foundations, wells, and petroleum/gas mining, there is no extant literature encountered in this research pertaining to the specific stresses induced by the drilling process on the surrounding soil, especially for auger drilled holes. This is likely due to the extreme variability of drilling conditions as well as skill and technique of the drill operator. What is known is that lateral earth pressures are reduced when shafts are excavated, which typically leads to a caving/sloughing type failure. It is unknown how much of the failure is generated by an instability of the soil mass itself as opposed to any stresses/vibrations the drilling process could induce.

A phone interview with Dave Judd (Judd, Dave. Personal Interview. 21 September 2012), chief estimator for Case Pacific Co., revealed that the standard of practice amongst drilling contractors for identifying caving/sloughing hazards consists of relying on local drilling experience while also looking at the density and the fines content of the sandy layer. Local experience usually takes precedent (i.e., having drilled close to the site before) over the information provided in the soils report if there exists a dominant local geologic formation that is well defined. If the site lies in an un-drilled region, the density of the soil and the fines content are used to identify potential hazards; loose and very loose layers of sand with less than 15% fines content are suspect and would likely be addressed as a caving/sloughing hazard. The methods currently employed in the industry for drilling on sites underlain by caving/sloughing hazards are limited to the use of drilling slurry, steel casing, a combination thereof, or pouring the concrete foundation through the tip of the auger used to drill the shaft, thereby never allowing the borehole to sit open and susceptible to caving/sloughing; The last method is known as Auger Casting and is an even more specialized subsector of an already specialized drilling industry.

Having spent a summer with Case Pacific Co., the author got to see firsthand the effects of positively identifying a caving/sloughing hazard. The cost of drilling tends to increase significantly for a number of reasons. First, there is more equipment involved in order to mitigate potential caving hazards. Large steel casings must be fabricated and mobilized to the site, as well as a casing driver attachment, so they may be advanced into the ground. If drilling fluid is used instead of steel casing, large tanks must be used and stored on site to hold, pump, and recirculate the drilling fluid; upon completion of the shafts, the drilling fluid must be disposed of in accordance with local regulations. Second, the time associated with drilling one shaft increases significantly when either fluid or casing is used, which leads to much higher operation costs. The auger must be detached from the drill rig and the casing driver must be reattached to spin and push the casing down after every few feet of drilling. When drilling fluid is used, the auger must be removed from the borehole more slowly in order to allow the drilling fluid to move down around the bit rather than overflowing at the surface; also, removing the auger too rapidly from a fluid filled hole can cause a low pressure zone to develop below and around the auger which can compromise the integrity of the hole

walls in that particular area. Fluid level must also be maintained in order to generate proper head pressures in the borehole. In the instance where the shaft is caving/sloughing and there are no means in place to mitigate the failure, a bulge forms in the shaft that must be filled with concrete. All of this leads to higher drilling costs and longer construction times.

The author spoke with Charlie Bower (Bower, Charlie. Personal Interview. 9 April 2014), a project manager with Case Pacific Co., about the implications of caving soil on the company's financial practice. Charlie said that nearly every project site must be evaluated for caving potential as it has significant impacts on project bids and budgets. The author and Charlie discussed, in detail, a recent project where a thick layer of sandy soil posed a threat to drilling operations as it was loose and below the 15% fines content industry cut off. Case Pacific Co. bid the project to include slurry drilling to counter the caving potential. When Case Pacific Co. arrived on site and began drilling, they discovered that the soil was far more resistant to caving than indicated by the information in the geotechnical report. Charlie postulated that the entire site could have been drilled without the aid of the slurry and he was kind enough to rework the bid documents retrospectively to demonstrate the financial impact this knowledge could have had. The total bid dropped over $500,000 on a nearly $4,000,000 project (over 12.5%); this was the result of shorter labor durations, less required equipment and fuel, and the removal of slurry from the project scope.

CHAPTER 3: EXPERIMENTAL AND LABORATORY TEST DESIGN

3.1 Introduction

The documents examined in the literature review indicated that it is not possible to consistently and accurately identify caving/sloughing hazards using the information that is currently supplied in a geotechnical report. The review did, on the other hand, reveal a number of relationships between soil strength and variety of other soil properties that will prove useful to the understanding of this research.

It is the overlying goal of this research to create a calibrated soil testing prototype that could identify caving/sloughing hazards without using a full scale test excavation. In order to achieve this goal, a series of laboratory tests were designed to create a calibrated and repeatable apparatus and schedule under which a variety of prototypes could be tested. The remainder of this chapter describes the logic and background behind how the testing regime was designed and implemented.

3.2 Testing Regime

It made a great deal of sense to examine closely those soil properties that the drilling industry currently evaluates caving/sloughing hazards with throughout the course of testing in order to more accurately define and describe these hazards in terms that can be easily applied to the industry at large; this indicated the fines content and density as variables in the testing regiment. I also speculated that the overburden pressure applied to the test soil would influence the propensity to cave/slough. The testing regime (see Figure 3.1: Testing Matrix) would include all three variables (density, fines content, and overburden pressure), but the sensitivity of the tests was specifically evaluated for two variables (fines content and overburden pressure).

First, the fines content of the test sand was incrementally increased to determine if the prototype in question could accurately discern one fines content from another. The fines contents of 0, 5,10,15, and 22% were tested. As mentioned before, 15% fines is an industry cutoff, below which the drilling contractor can be weary of sand caving; therefore, a range of fines contents was selected to determine the sand's behavior leading up to the cutoff and beyond in an attempt to evaluate a behavioral shift in the sand-fines mixture as the fines content increased. Second,

vertical overburden pressure was applied and increased incrementally for each fines content to simulate varying depths. A series of vertical overburden pressures was applied to the test soil for each fines content increment. The test is only applicable to sand layers above the water table at depths typical of deep foundation drilling; therefore, pressures were applied to simulate in-situ earth pressures at depths of approximately 5, 10, 20, and 40 feet below the surface. To accomplish this, a large lever arm loading apparatus was created (see 3.3.2 Loading Apparatus). Lastly, the density of the sand being tested was determined through the method by which the sand was placed in the test apparatus. The density varied as the fines content and overburden pressure changed. The density of the test sand was not strictly regulated, but rather, the placement process (see 3.4 Sample Preparation) used to fill the test chamber and the overburden pressure applied to that particular trial determined the density. The placement process was the same across all tests, which generated a loose or very loose condition with a highly flocculated soil fabric; however, the test sand densified with the application of the overburden pressure, more so under higher overburden pressures. The density of test sand in this research ranged from 86 lbs/ft^3 for clean sand (0% fines content) under the lowest overburden pressure up to 117 lbs/ft^3 for sand containing 22% fines under the highest overburden pressure tested. It should be noted that the aforementioned densities are wet densities (see 3.3.5 Water Contents for Testing).

Percent Fines & Gravimetric Water Content

Overburden Pressure	5' / 36KPa	10' / 60KPa	20' / 121KPa	40' / 216KPa
0% FC 3.5% WC	3	3	3	3
5% FC 5.12% WC	3	3	3	6
10% FC 7.7% WC	3	2	2	2
15% FC 9.52% WC	2	2	3	2
22% FC 9.9% WC	3	2	2	2

Number of Trials Performed

FIGURE 3.1: Testing Matrix

3.3 Test Design

3.3.1 Sand and Fines

To ensure the repeatability of the test results with the potential for future testing in mind, the author selected a sand that is widely available for retail purchase. #20 Silver Sand was purchased in 100 lb bags from P.W. Gillibrand Co. Inc. to serve as the test sand. The author conducted a grain size analysis on two different bags to ensure product uniformity. The sand, classified as “Poorly Graded Sand” and falling under the group symbol SP, is light tan in color, sub-angular in shape, and has a specific gravity of 2.6. According to the grain size distributions seen in Figure 3.2, #20 silver sand had a coefficient of curvature of 1.0 and a coefficient of uniformity of 1.6. The mean particle size (D50) was 0.7 mm.

As with the sand, a widely available silt was selected to ensure test repeatability. A finely ground silica flour, known as Sil-co-sil 52, was purchased in 50 lb bags from US Silica to serve as the test fines. A hydrometer test conducted using the silica flour confirmed that the particle size distribution was “silt-like”. The results of the hydrometer test can be seen in Figure 3.3 overlaid with the M.I.T, CFEN, ISO/CEN fines classification system. The silica flour, classified as “Silt” according to the USCS and falling under the group symbol ML, is white in color and non-plastic in behavior.

When prototype testing began, the test soil was clean sand at 0% fines content and was classified as SP: Poorly Graded Sand. After the first round of testing was completed, Sil-co-sil 52 was added to the clean sand to generate fines contents of 5 and 10%. This mixture produced a soil that was classified as SP-SM: Poorly Graded Sand With Silt. Then, more Sil-co-sil 52 was added to achieve fines contents of 15 and 22%, which was then classified as SM: Silty Sand according to the USCS.

3.3.2 Loading Apparatus

In order to simulate in-situ earth pressures under laboratory conditions, the author designed and fabricated a lever-arm loading device to apply vertical overburden pressure to the test soil. The pressure applied to the soil remained essentially constant regardless of how much the soil deflects when reacting to the load. A panoramic image of the device can

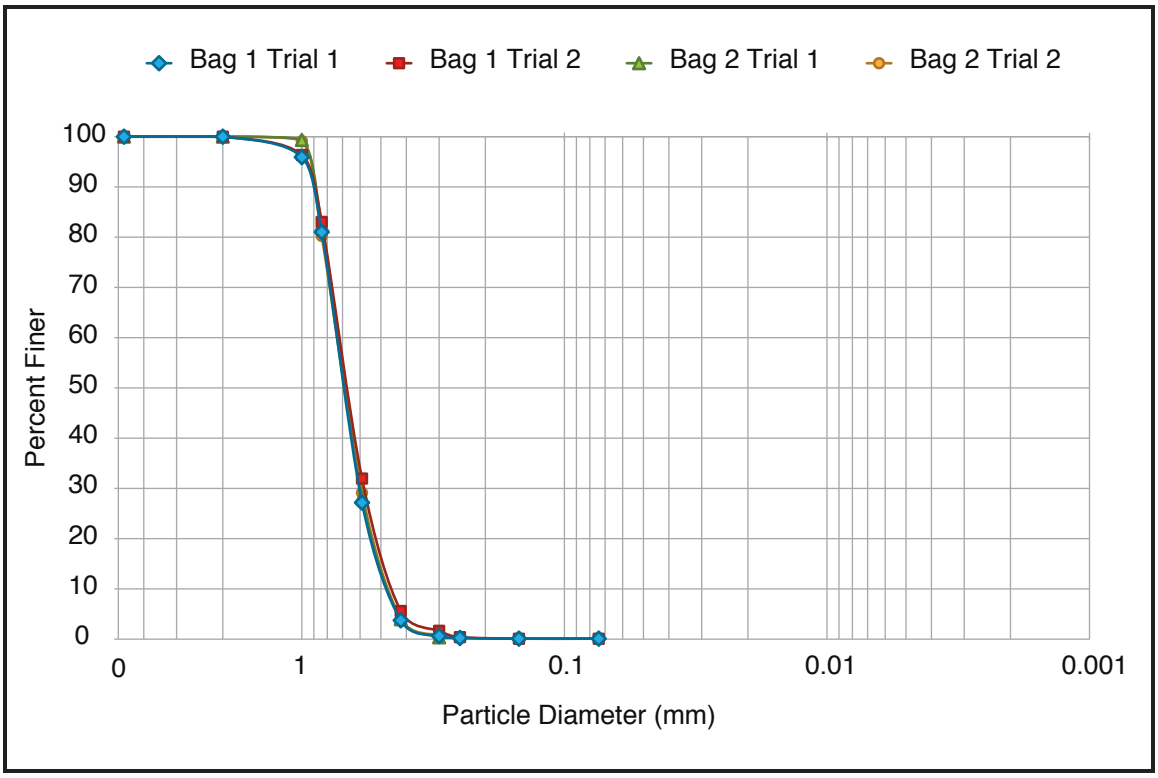

FIGURE 3.2: #20 Silver Sand Grain Size Distribution

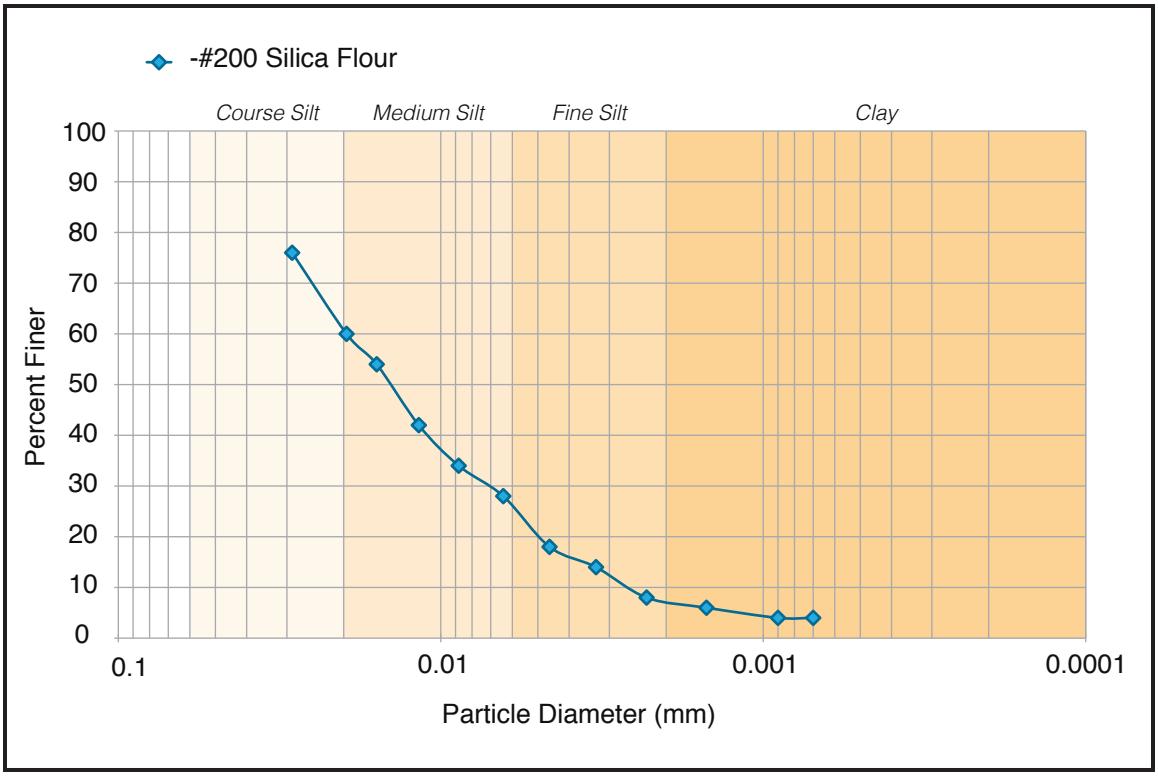

FIGURE 3.3: -#200 Silica Flour Grain Size Distribution

be seen below in Figure 3.4. The devise consisted of a rigid steel frame and heavy steel plate foundation that were capable of resisting the anticipated loads without requiring outside support. Two 10 ft long beams attached to the frame with pin connections, allowing the beams to pivot freely and act as the lever-arms. Steel pressure plates (weighing approximately 50 pounds) hung from the ends of the 10 ft beams using a platform and chains generated a reaction force below the frame with a large mechanical advantage. This force was transferred through bolts below each beam and into a steel plate that distributed the load evenly over the surface of the test soil contained within a large cylindrical tub, centered below the frame.

FIGURE 3.4: The Constructed Loading Device in the Lab

3.3.3 Cone Sizing

The prototype soil-testing devices were designed to be used in conjunction with a Cone Penetration Test (CPT). First, the CPT is conducted when the rig hydraulically advances lengths of steel rod into the ground instrumented with a pressure-sensing cone at the end, followed by a friction-sensing sleeve. When the target depth is reached, the steel rods are pulled out of the ground, leaving a test hole. A steel dummy cone (no load sensing instrumentation) was machined to mimic the exact shape and size of the cone penetrometer for use in lab-based trials.

A 10 cm^2 cone (1.46 inches in diameter) was the initial target size to generate a test hole for

the prototypes; however, after talking to a representative with Fugro (a geotech consulting firm), it was brought to my attention that, even if a 10 cm^2 cone is used to conduct the soils exploration, the hole left by the test would be 15 cm^2 (1.72 inches in diameter) because a short step-out is placed a few feet behind the cone as it is advanced. The step-out increases the diameter of the hole such that the 10 cm^2 rods following the step-out are no longer in contact with the hole walls, which reduces the overall effort required to push the cone to greater depths. When a 15 cm^2 cone is used for the soil exploration, the rods used to advance the cone are stepped inward to achieve the same effect. As a result, the dummy cone used in lab trials was lathed to 15 cm^2 (1.72 inches in diameter) with a 60º conical tip and the testing prototypes were designed for this diameter.

3.3.4 Boundary Conditions

In order to conduct tests under various overburden pressures and fines contents in a repeatable manner, a container had to be designed that would confine the sand while not adversely affecting the test results due to boundary conditions. According to De Ruiter (1981), for over-consolidated and normally consolidated loose sand, the boundary effects induced by a confining chamber on cone penetration are negligible at, and beyond, a diameter ratio (diameter of testing vessel divided by the diameter of the cone) of about 20. De Ruiter also stated that the results apply to vertical boundaries as well. Knowing that the standard CPT rod is a 15 cm^2 cross section (1.72 inch diameter), the confining chamber must be approximately 34 inches tall and 34 inches in diameter.

A drop-section of steel drill casing was donated by Case Pacific Co. in Paso Robles, CA to serve as a test chamber. The steel casing was 30 inches in diameter and 29 inches tall. Although the horizontal and vertical diameter ratios are closer to 17 for this chamber, the data presented by De Ruiter (sampled from Parkin 1977) seen in Figure 3.5 suggests that the boundary effects on cone penetration will also be negligible at this ratio. A study by Yang et al. in 2014 reinforced this assumption.

3.3.5 Water Contents for Testing

No extant research can predict the moisture content that a soil will contain when encountered

underground, as there are far too many variables that influence this ever-changing soil condition; as a result, the author designed a series of tests to determine how much moisture the test soil (described in 3.3.1 Sand and Fines) would reasonably contain if it were encountered out in the field. Because the prototype is only being tested in scenarios where sand is found above the water table, there are at least two ways in which moisture can reach a layer of sand: capillary rise and downward percolation. The tests were designed to evaluate expected water contents of soil subject to these two forms of water movement in samples containing 5,10,15, and 20% fines. A total of eight test specimens were prepared (four capillary rise and four percolation), each contained within a plastic tube approximately 3 inches in diameter and 18 inches tall with an open bottom. The sand and silica flour was mixed by stirring the two dry ingredients in the required proportions, and then pluviating the mixture into each tube using a funnel.

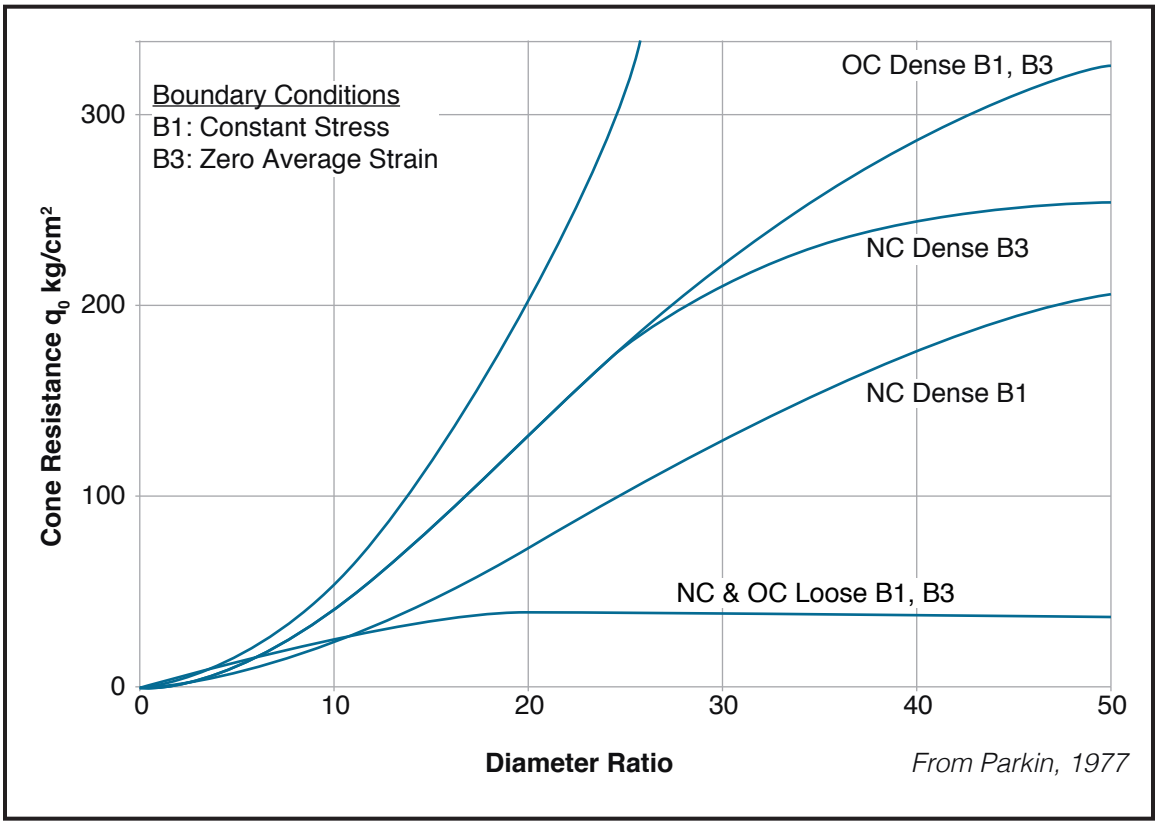

FIGURE 3.5: Effect of Chamber Diameter on Cone Resistance

The capillary rise tubes were placed in a tray and the tray was then filled with 2 inches of water. The tray was filled periodically to maintain 2 inches during capillary rise. The samples remained in this state for several days.

The percolation test specimens were poured into tubes with permeable 2-inch tall false bottoms. Then, a series of hoses and stopcocks were used to drip water onto the sand mixture exposed at the top of each tube at a rate of one drop per second. The drip rate

FIGURE 3.6: Capillary Rise and Percolation Test Setup

was set to ensure that the water would saturate each specimen without causing the fines to migrate downward. Water was applied in this manner until each mixture reached its maximum field saturation and an appreciable amount of water passed through the false bottom. The test setup can be seen in Figure 3.6.

When the percolation tests were complete, all eight specimens remained in this state for one week; 2 inches of water was maintained in the capillary rise tray over the course of this week. Special segmented sampling scoops were constructed to be able to extract the sand mixture from each tube accurately in 3-inch depth increments. Samples were weighed,

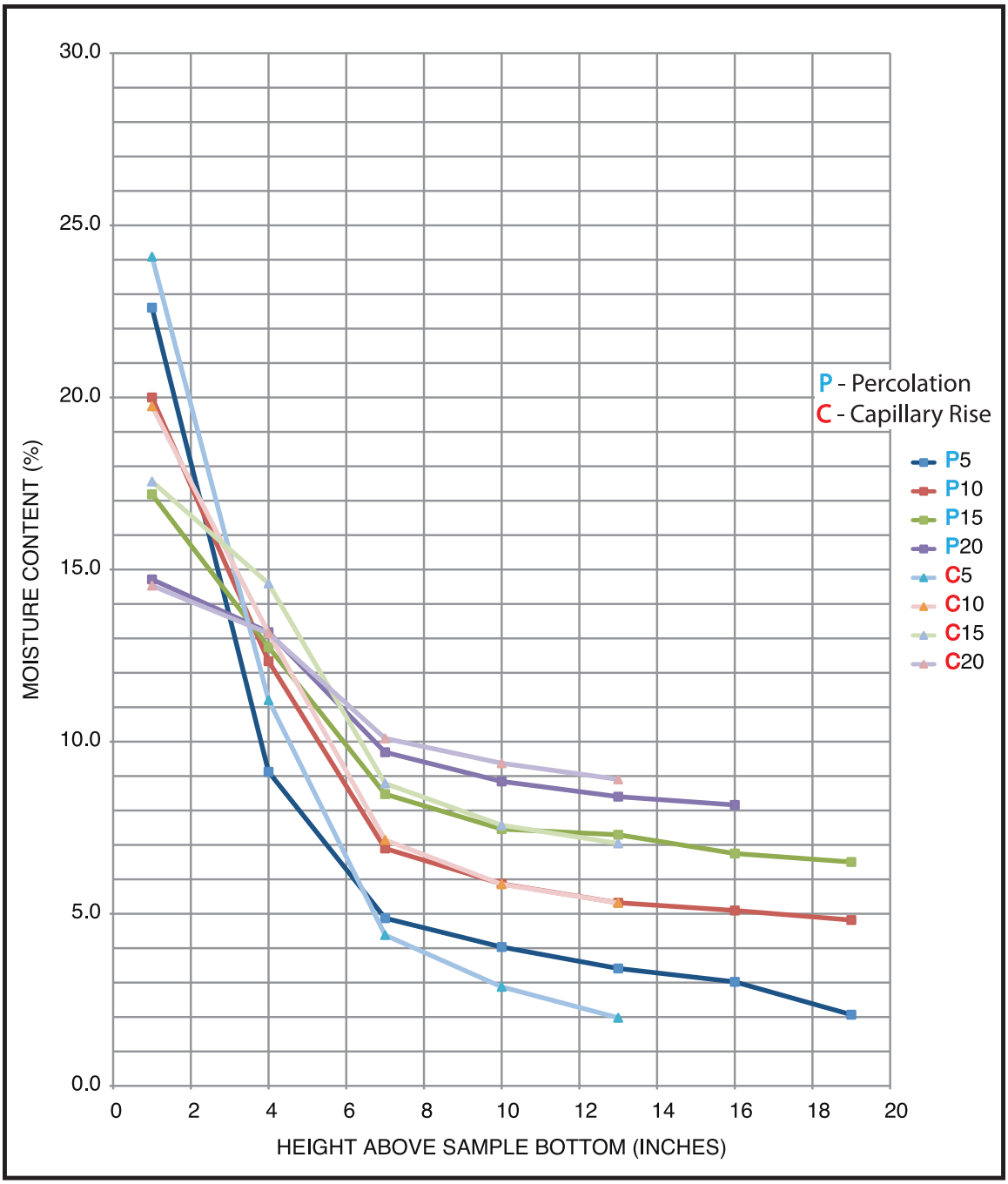

FIGURE 3.7: Results of Moisture Content Testing

oven dried, and logged to graph water content as a function of distance above the bottom of each test specimen (height 0 was 2 inches from the bottom of all eight tubes to eliminate the fully saturated sand in the capillary rise specimens and the false bottom of the percolation specimens). The results of these tests can be seen in Figure 3.7.

Ideally, the results from the two different test methods would simply be averaged for each fines content to determine an appropriate water content, but other soil parameters required consideration. Ultimately, the water content for each stage of testing was determined by the average of the two tests at a given fines content taken 7 inches from the bottom of the tube with an additional 10% water added (ie – gravimetric water content x 1.10). The 10% increase in water added was enough to satisfy all surface charges of the silica flour and was required to be able to mix the fines into the sand more effectively. This strategy is discussed in Section 3.4.2 Mixing in greater detail.

3.3.6 In-situ Stress

In the early stages of development, the author postulated that defining the stress state of the test sand during and after cone penetration takes place would be useful in designing a prototype to generate a failure in the test sand. Attempts to define these stresses were informed by numerous articles from the proceedings of the ASCE national convention in 1981 that focused exclusively on cone penetration testing. Soil deformation patterns around cone penetrometers were postulated and the associated failure mechanisms were proposed. The deformation patterns and failure mechanisms found in these articles closely resembled the deformation patters and failures associated with driven foundation piles presented by Sowers (1979).

Attempting to define the stresses associated with these processes led to Vesic's cavity expansion model. The expansion of a cylindrical or spherical cavity in the soil medium can more accurately predict the resistances one might expect when attempting to push a cone penetrometer but, according to Rohani and Baladi (1981), the model cannot "… accurately predict the state of stress and strain within the soil medium during the penetration process." In order to use the cavity expansion model, the cohesive strength, internal angle of friction, density, and shear modulus of the soil must be known. For this thesis, many of these properties could change drastically throughout the course of testing; therefore, the cavity expansion model was not applied to this research.

Instead, a graphical representation of the stresses induced by cone penetration was constructed in q-p space (as seen in Figure 3.8) to better comprehend these stresses. A

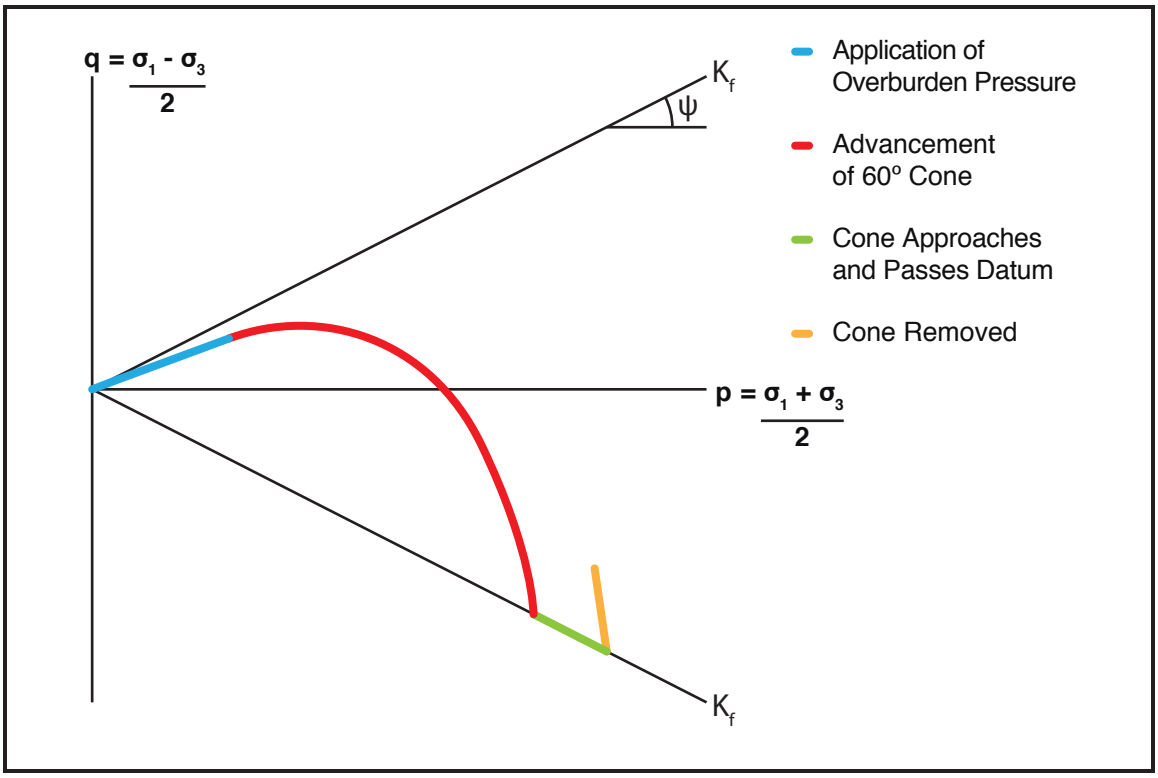

FIGURE 3.8: Theoretical Load Path

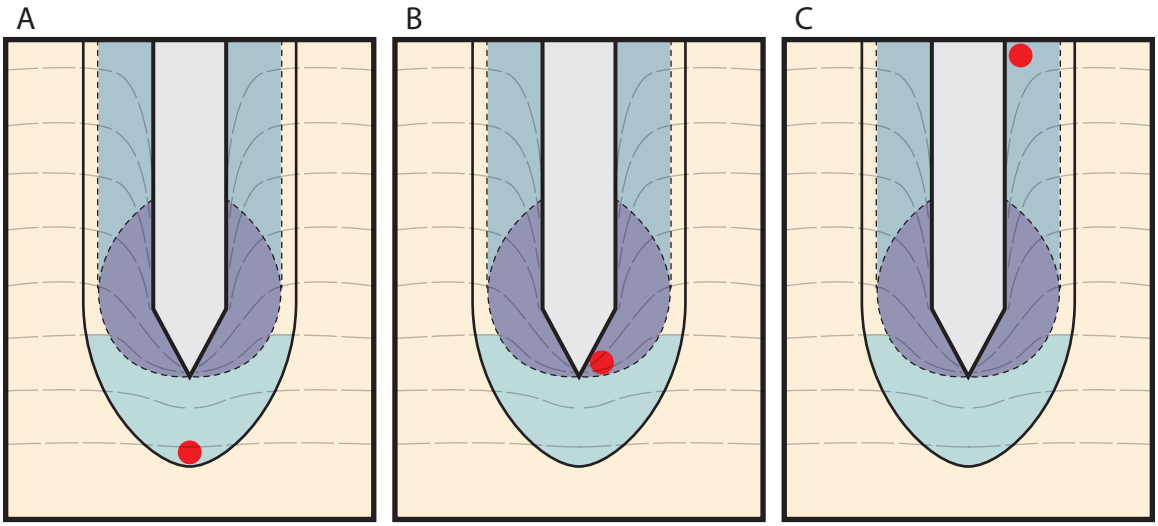

Undisturbed Zone
Pre-Compressed Zone
Previously Disturbed Zone
Direct Disturbance Zone
when cone passes Point X (shown in red)
Reference Datum

FIGURE 3.9: Pattern of Soil Deformation During Cone Penetration

progression of cone penetration relative to a target datum, seen in Figure 3.9 as adapted from Muromachi (1981), assists in explaining the stress path during the various stages of cone penetration. The approach of the cone and subsequent pre-compression, seen in Figure 3.9A, in q-p space is linear with σ_1 (vertical stress) increasing twice as fast as σ_3 (horizontal stress). When the cone reaches the datum, as seen in Figure 3.9B, the pitch of the 60º conical tip begins adding additional horizontal stress until σ_3 is nearly three times σ_1. The stress increases in this manner until the soil is sheared and pushed aside to allow the cone to pass. When the cone has passed the datum and penetration continues, as shown in Figure 3.9C, there is no change in the stress state until forward penetration stops and the cone is removed. When the cone is reversed and backs out of the test hole passed the datum, σ_1 and σ_3 are both reduced.

3.4 Sample Preparation

3.4.1 Materials

Lab trials at the scale discussed in 3.3.4 Boundary Conditions required the acquisition of 1100 pounds of #20 Silver Sand and 250 pounds of Sil-co-sil 52. The test soil was stored and sealed in 5 gal buckets to preserve the water content of the sand-silt mixture after it was prepared and between tests. The buckets made it easier to move the test soil around the lab and pour the mixture in manageable increments.

3.4.2 Mixing

The author used a small cement mixer to mix the sand, silica flour, and water together. Only two 5 gal buckets of soil could fit in the mixer at any given time; therefore, bucket proportions were calculated and mixed individually to produce a more homogeneous test soil.

No problems were encountered when mixing water into the clean sand for testing at 0% fines; however, the first attempts at mixing silica flour into the sand resulted in an undesirable mixture. First, the moist sand and the entire silica flour supplement were placed in the mixer and the opening of the mixer was sealed with plastic wrap to prevent airborne losses of silica flour when mixing. The mixer was turned on and allowed to run for a few minutes. Unfortunately, the silica flour was not coating each sand particle, but was clumping instead.

Further mixing, in an attempt to let the mixture homogenize, only exacerbated the clumping. A different strategy was required.

In an attempt to distribute the silica flour more evenly through the moist sand, dry silica flour was slowly sprinkled into the moist sand as the mixer was running. This greatly reduced the formation of silica flour clumps and was deemed acceptable for testing, though it would ultimately prove to be inadequate. The clumps that remained were broken apart during the sample placement process (see 3.4.3 Placement). This method of mixing was abandoned after many lab trials demonstrated that the test soil was gradually gaining strength between tests. Because the silica flour was dry when it was added to the wet sand, some of particles were not fully hydrated even after mixing. When the sand was removed from the test chamber, placed in buckets, and reused for the next test, the sand would mix and expose the drier silica flour to more free water that was coating the sand particles. The surface charges of the silica flour would bond with the water and the test soil would increase in apparent strength. Instead of generating a series of tests to determine if the sand could to be further mixed to exhibit constant strength properties, a new mixing method was developed.

The third and final method of sample preparation was very effective and was used to mix the test sand for all stages of testing. Water was added directly to the silica flour in proportions large enough to generate a thick liquid. As mentioned before, the amount of water added to achieve this liquid was calculated as the average of the capillary rise and the percolation results at 7 inches from the bottom of each test multiplied by a factor of 1.10. For example, moisture content tests indicated that 4.65% gravimetric water content was an appropriate testing wetness for the mixture containing 5% fines, but this was multiplied by 1.10 to accommodate mixing, yielding a moisture content of 5.12% instead. Although this increase seems rather small, because the fines are non-plastic, the additional water was enough to push the fines across the liquid limit threshold and ensure that the silica flour was fully hydrated and fluid at the time of mixing. A small hand-pumped garden sprayer was used to pressurize the mixture and spray it into the moistened sand that was tumbling in the cement mixer. Although very time consuming and messy, this method all but eliminated the formation of silt clumps and generated a test soil that did not change with time.

3.4.3 Placement

The term ‘pluviation’ can be seen with great frequency throughout any work that discusses CPT calibration. Pluviation is a process in which dry sand falls through a series of dispersion grates and into the test chamber in such a way that each sand particle falls at the same velocity and from the same height. The height and velocity of falling particles determines their impact energy as they fill the test chamber, which is directly related to the relative density of the newly generated test soil. Following a prescribed pluviation process helps to ensure a homogenous test soil. Because this thesis is aimed at calibrating a prototype soil-testing device, the uniformity of the test soil from one trial to the next was paramount.

A welded circular frame, whose diameter was slightly smaller than that of the testing chamber, was fabricated with four layers of 1/4-inch steel mesh in the center. The loading apparatus was outfitted with a series of pulleys and steel cable attached to the circular framer with a crank and lock system that could raise, lower, and lock the frame at a given height within the test chamber. With this setup, the test soil could be poured from buckets onto the mesh and fall into the test chamber from a predetermined height. This process, although similar to pluviation, cannot be referred to as pluviation because pluviation is a process reserved for dry sample prep, but the soil used for thesis testing was very moist. Attempting to truly pluviate the moist test soil proved futile, but the principles were still valuable in generating a homogenous test soil from trial to trial.

The fall height of the wet pluviated test soil was less critical in these tests due to the application of an overburden pressure after the chamber was filled. Any variation in fall energy was assumed to be negligible when compared to the densifying effect of the applied load. More importantly, the grate would break apart clumps that formed during the mixing process. An image of the grate and rigging can be seen above in Figure 3.10.

3.5 Lab Trial Procedure

The author developed and tested a number of prototypes throughout the course of this research, but most of them were deemed inadequate before reaching full-scale lab trials. This section succinctly outlines the procedure of setting up and running a lab trial with Prototype 9 (the last and most effective prototype developed). A detailed description of prototype development can be

FIGURE 3.10: Pluviation Apparatus

found in Chapter 4 and in Appendix A . Refer to Figure 3.11 for graphic aid.

First, the test chamber was centered under the loading frame using guide lines drawn on the base plate. The distribution grate was placed in the bottom of the test chamber and the cable rigging was arranged under the loading frame to move the grate up and down. Then, the author misted the entire inside of the test chamber with water to prevent the loss of water from the test soil to the chamber perimeter.

Next, the author poured the prepared test soil out of the storage buckets onto the elevated grate and pushed the soil through the steel mesh. When the chamber was nearly full and the grate was pulled up to the rim of the test chamber, the rigging and grate were removed. The chamber was then topped off by hand and scraped flush. The author used a shop crane was used to lift the top plate and place it on the test soil. The dummy cone was threaded through the loading frame and clamped in place to assist in centering the top plate under the frame; verifying measurements ensured that the lever arms were seated on the load transfer bolts at equal distances. This distance relates to the mechanical advantage the lever arms can achieve and must be equal on both sides to ensure a uniform load of known magnitude.

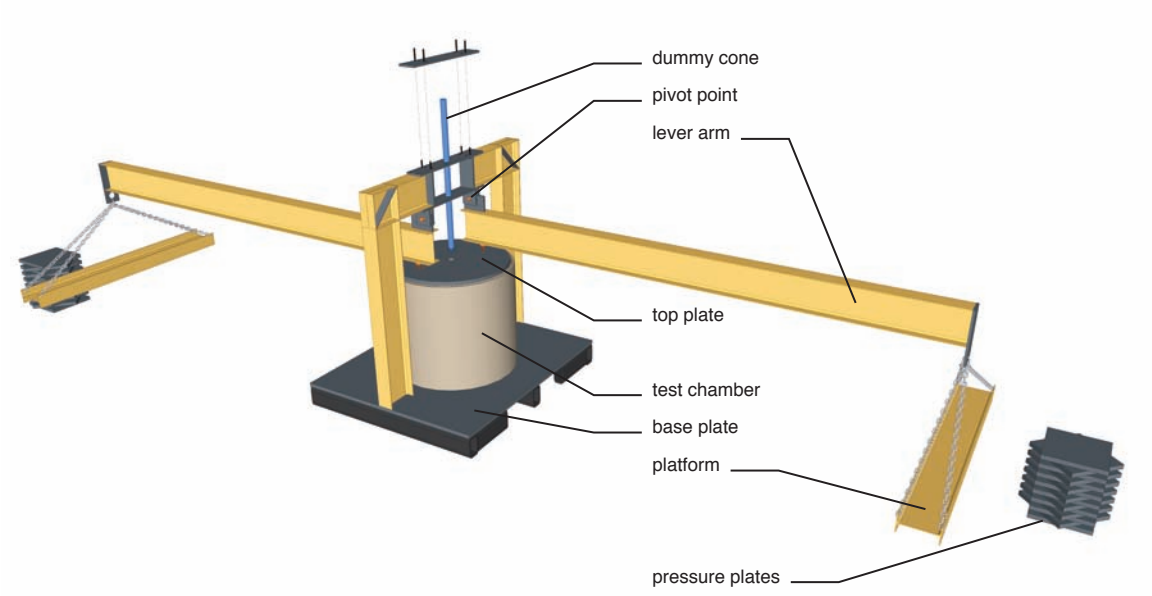

FIGURE 3.11: Schematic of Loading Device

The author used two shop cranes simultaneously to pick up the 10 ft lever arms and hold them in place under the loading frame as the pin connections were made. The load transfer bolts were backed out of the distribution plate to engage the bottom of the lever arms as the arms were lowered. The cranes were disconnected from the lever arms and moved to the end of the arms where they were reattached using a heavy cable sling. The pressure platforms were then attached to the lever arms and any steel pressure plates were placed on the platform (the number of plates was governed by the target overburden pressure for that specific test). The cable slings and cranes were used to lift the arms so that the transfer bolts could be raised/lowered; the bolts

needed to be positioned in such a way that when the cranes were fully disengaged, the lever arms were parallel to the ground and level because the loading apparatus was calibrated in this position (see 3.6 Additional Documentation).

When the load was fully supported by the test soil within the chamber, the author slowly advanced the dummy cone via a hydraulic jack until it nearly touched the base plate. The author then backed the dummy cone out of the test soil via the same jack and removed from the apparatus, leaving a clean test hole. The author was then able to lower Prototype 9 into the hole and attach it to the pneumatic pressure vessel that was pressurized to 100 psi. The prototype was manually opened and the pressure was released from the pressure vessel and allowed to fully dissipate before closing the prototype. Upon closing the prototype, it was removed from the hole and disassembled in order to extract and weigh any collected test soil. The collected soil was placed in an oven to dry as the entire apparatus was broken down. The author removed the test soil from the chamber and returned it to the storage buckets to preserve the water content until the next test could be run.

3.6 Additional Documentation

A few other tests were conducted throughout the course of the data collection that were not explained above. First, the loading apparatus required calibration testing to know with confidence the magnitude of the loads being applied. The resulting load calibration plot that was subsequently used throughout the course of testing to determine the load being applied to the test chamber can be seen in Figure 3.12. Second, water content samples were taken each time the fines content or applied load was changed to ensure soil uniformity across tests. When it came time to adjust the fines content, the author tested the water content of every individual bucket to determine the appropriate amount of water to add in the mixing process. The samples collected in the moisture tins were then reused to double check the fines content after the round of testing was complete. The dry samples were emptied into a tray and the aggregate sample was weighed before it was washed through a #200 sieve and re-dried to determine the amount of fines the test soil contained. None of the results conflicted with the original intent of the test soil component proportions.

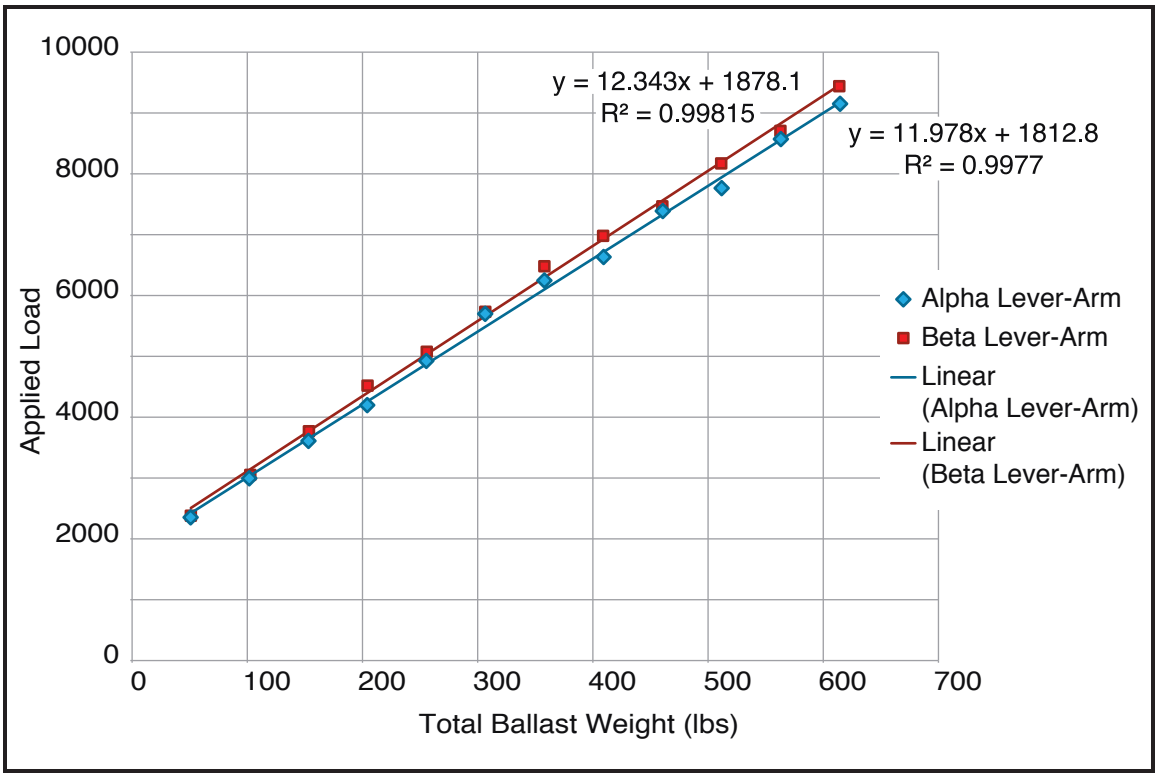

FIGURE 3.12: Loading Apparatus Calibration Plot

CHAPTER 4: PROTOTYPE DESIGN AND DEVELOPMENT

This chapter outlines the sequence and logic behind the prototype development that took place throughout the course of this research, ultimately concluding with a detailed description of the ninth and final prototype known henceforth as the Pneumatic In-situ Soil Caving Index Sampler, or PISCIS. For a more complete description and analysis of each prototype developed in this research, see Appendix A.

4.1 Prototype Development

Prototype design began by examining the project goal: Create a soil sampling device that could fit down an expired CPT hole to directly test the surrounding soil for its propensity to cave. The first developmental decision pertained to the method of direct soil testing that would be used. Would the prototype collect a sample via physical or mechanical abrasion, vibratory stimulation, pressure or vacuum disruption, or by pneumatic agitation?

Collecting a physical sample using mechanical abrasion appeared to be the most reliable and repeatable means of testing. A series of small tubular prototypes were developed that could fit inside of an expired CPT test hole. Once inside of the test hole, a triggering rod could be advanced downward within the prototype causing steel prongs contained within the tube to open and dig into the sand surrounding the prototype. It was thought initially that cutting into the hole walls with these prongs would cause planes of weakness to form within the soil mass that would lead to a shear failure of the hole walls. The affected soil would “slough” off of the hole walls in whatever volume the strength of that particular soil would allow, falling directly into the sample collection tube below the prototype. After varying the size, orientation and number of triggering prongs the mechanically activated prototypes were deemed insufficient due to a lack of sample weight collected in addition to difficulties in trial repeatability. By carefully excavating down to the area of test soil that was affected by these prototype trials, it was apparent that, although the mechanical triggers were in fact cutting into the surrounding soil, the soil required a more aggressive form of agitation in order to cause an instability/failure within the soil mass.

The author postulated that using pressurized air instead of a mechanical trigger would generate a more versatile and adaptable prototype. The mechanical prototypes were difficult to construct

and could not be adapted once built. With a pneumatic prototype, the size, shape, number, and orientation of the nozzles expelling the pressurized air into the test hole could be easily varied without having to rebuild the prototype entirely. Most importantly, the pressure with which the air was expelled could be regulated, making it easy forcefully agitate the surrounding soil based on the results. Another motive for moving toward pneumatic prototypes originated from the inability to keep the mechanical prototypes centered in the test hole while running trials, which resulted in high degrees of variability in the test results. A pneumatic prototype, hypothetically, would not move within the hole while the pressurized air was expelled, thereby increasing test repeatability.

The first pneumatic prototypes that underwent testing yielded promising results in terms of sample weight collected. When the air pressure was increased or decreased during these tests, the sample weight collected varied accordingly (increasing with increasing pressure and decreasing with decreasing pressure); this bolstered the prospect of creating a pneumatic prototype that was capable of testing a wide variety of soil types with great accuracy. Collection weights from pneumatic trials, although high, varied upwards of 25% from one trial to the next. The source of this variation was identified after running trials in shallow holes where the test could be observed more easily. Not all of the soil dislodged by the pressurized air was falling into the collection vessel below and, as the prototype was being removed from the hole, the sample within the collection vessel was contaminated with other soil accidentally scraped from the hole walls. Efforts to contain ALL of the dislodged soil while also preserving the collected sample as the prototype was brought to the surface decreased the variability between tests. As the motivation for sample containment and preservation continued to drive design evolution, the test results varied progressively less and the final prototype was developed. This prototype, known as the PISCIS, underwent extensive laboratory trials and is cornerstone of this research.

4.2 Prototype 9 (PISCIS)

4.2.1 Description

Prototype 9 (see Figure 4.1) is a split tube pneumatic sampler that was machined out a solid, cold-rolled, carbon steel rod. The catchment tube (lower half of the split tube) is 1.69 inches in diameter and has a truncated 60^{o} conical tip. The lid is also 1.69 inches in diameter and

has a truncated 60º conical top to assist in removing the device from the test hole. The lid fits tightly with the catchment tube to be able to completely seal the PISCIS as it is placed in the test hole and after the test is run, preserving sample integrity and guaranteeing test repeatability. A series of screened ventilation tubes allow the pressurized air to escape up and out of the test hole while collecting the soil that may be in aeolian suspension. The PISCIS is advanced into the test hole in the closed position (Figure 4.1A), where the split tube is then opened (Figure 4.1B) to expose the nozzle that expels the pressurized air to a portion of the hole walls. The pressurized air is then released from the pressure cell and, when the air has dissipated, the lid is returned to the closed position before the PISCIS is removed from the test hole. Only the soil that was directly affected by the pneumatic agitation is captured and contained within the PISCIS after the trial, which is a drastic improvement on previous prototypes.

FIGURE 4.1A: Prototype 9 Closed

FIGURE 4.1B: Prototype 9 Opened

CHAPTER 5: TEST RESULTS AND DISCUSSION

A total of 59 laboratory trials were run using the PISCIS. The samples collected were weighed, oven dried, and reweighed. Due to trial complications and sample loss during lab analysis, 51 of the 59 samples provided data points for further analysis and discussion in the following sections. The ultimate goals of the PISCIS lab testing were to demonstrate the functionality of the prototype and generate a calibration curve of sample weight collection developed in a controlled environment.

5.1 Test Results

The two conditions that varied throughout the course of testing were fines content (FC) and applied effective overburden pressure (σ_v'). The moisture content of the soil mixture was incrementally increased throughout testing, but this was not considered a primary test variable as the increases were proportional to increases in the fines content (3.3.5 Water Contents for Testing and 3.4.2 Mixing). Collected sample weights were plotted as a function of fines content and the results can be seen in Figure 5.1. Collected sample weights as a function of applied overburden pressure were also plotted and the results can be seen in Figure 5.2. Water content of the bulk test sand was also recorded and plotted as a function of the fines content being tested to verify consistent conditions throughout the course of testing. This plot is presented in Figure 5.3.

5.2 Discussion of Results

The primary design goal during prototype evolution was to create a device that could collect a broad range of sample weights when varying both the fines content of the test sample and the applied overburden pressure. The breadth of sample weights collected during lab trials suggests that the PISCIS *is* capable of distinguishing between a variety of in situ scenarios generated in a lab settings. A more detailed discussion of the relationships uncovered during testing and their implications are discussed in the following sections.

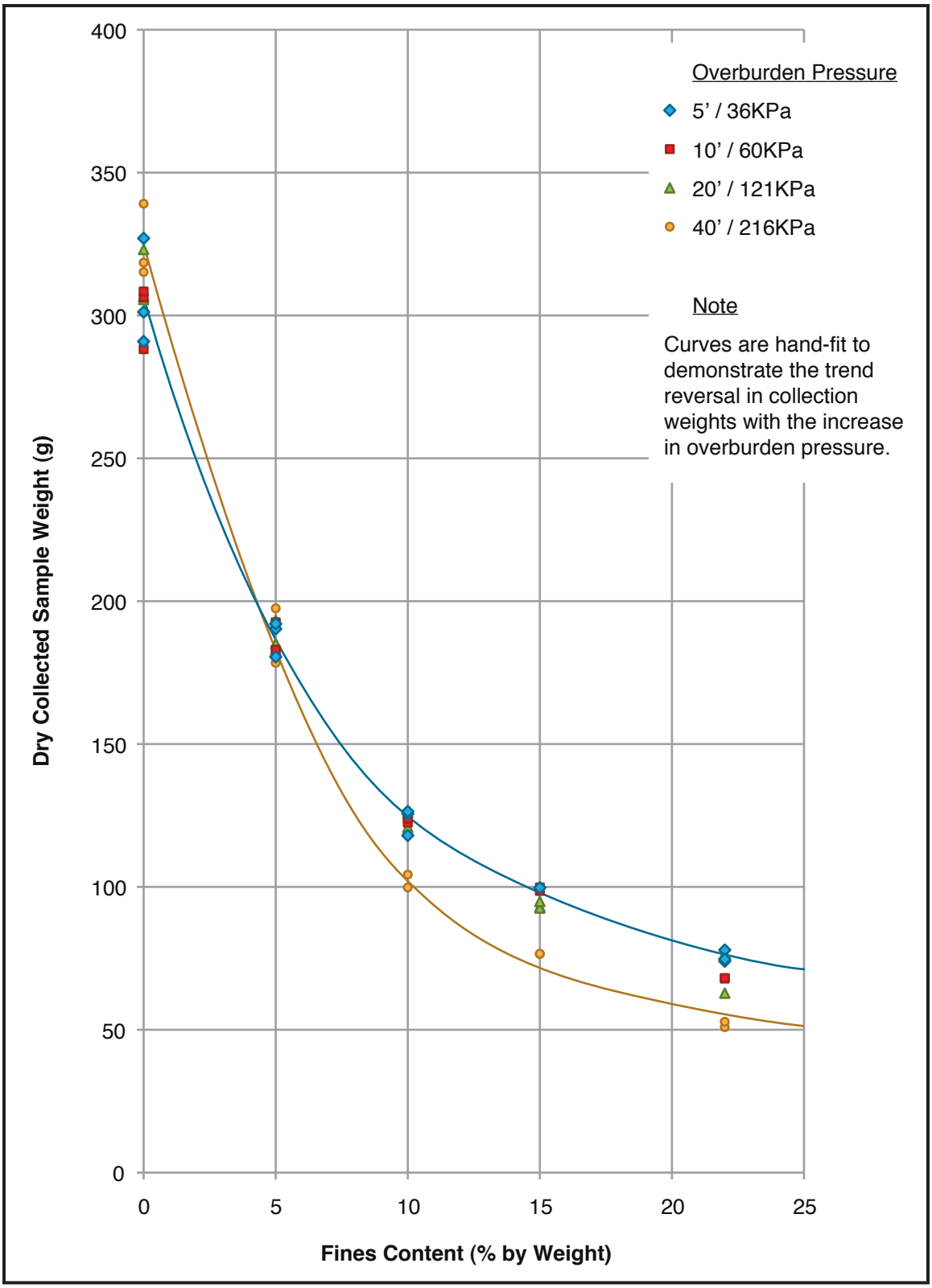

FIGURE 5.1: Yield As A Function of Fines Content And σ_v'

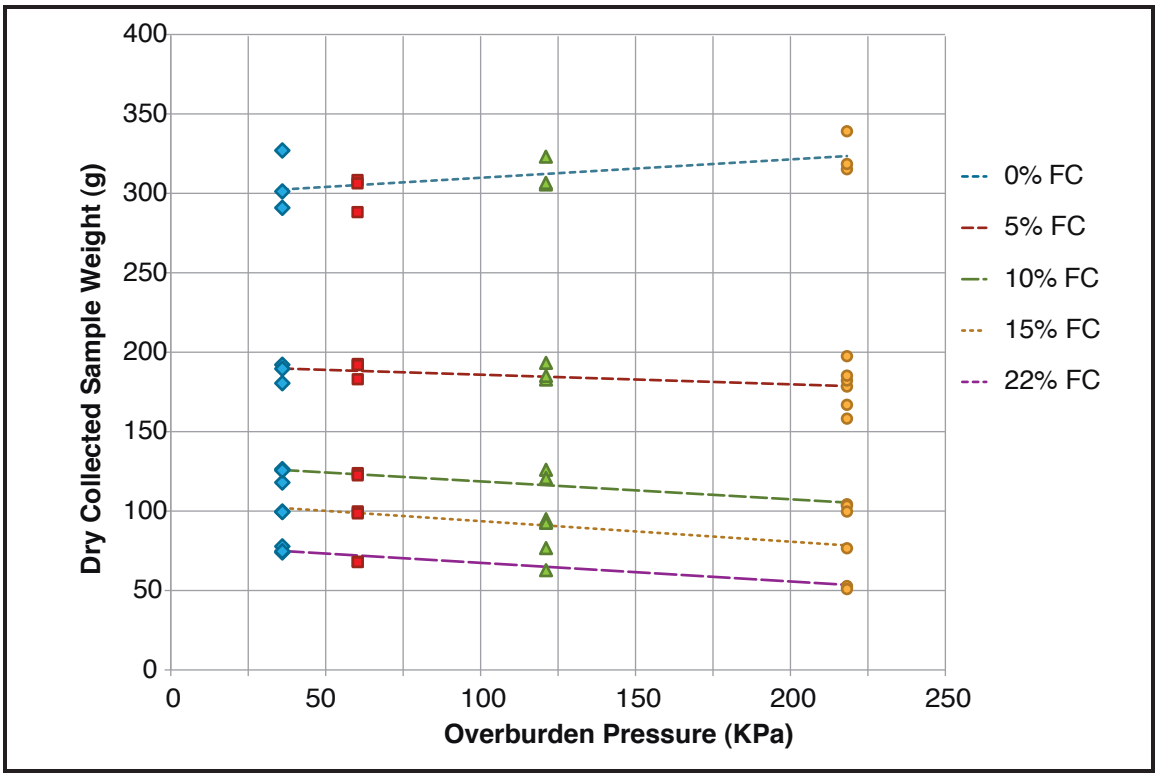

FIGURE 5.2: Effect of Overburden Pressure

5.2.1 Fines Content and Collected Sample Weight

The data displayed in Figure 5.1 indicates a correlation between collected sample weights and fines content of the test sand. The relationship appears to be approximately exponential in nature. The largest sample weights were collected during tests run at 0% FC with a mean collected sample weight of 311 grams. Collection weights decreased with the addition of non-plastic fines to a mean collected sample weight of 66 grams for tests at 22% FC. Although the specific nature of the correlation between fines content and collected sample weight was unknown before lab testing, the existence of some type of correlation was postulated simply due to the current drilling industry method of identifying caving hazards. The greater the FC of a sandy layer encountered in a soils report, the less likely that layer is to cause concern amongst drilling contractors (Judd, Dave. Personal Interview. 21 September 2012). This implies that the addition of fines to sand increases the strength of the mixture until it is no longer a caving hazard.

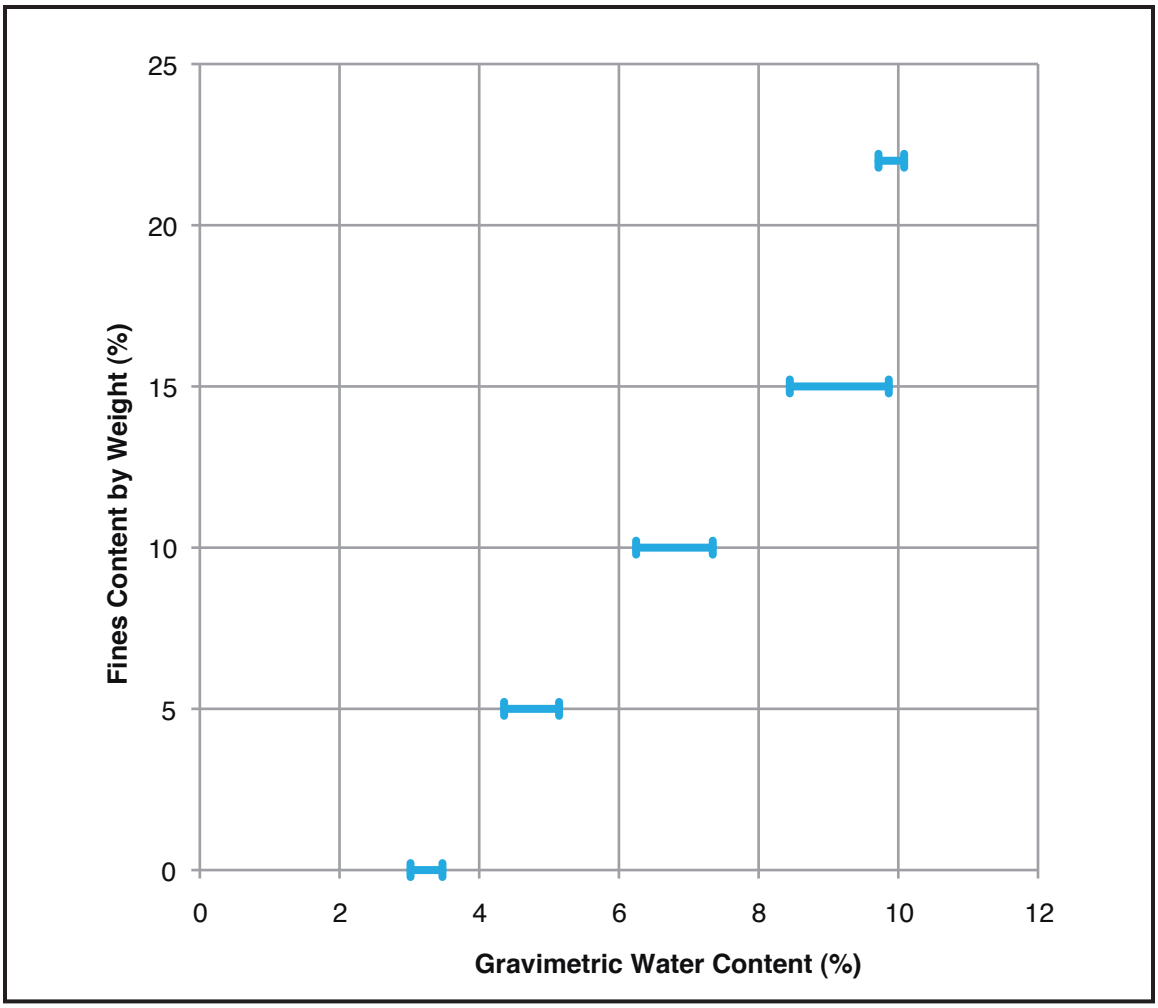

FIGURE 5.3: Water Content Ranges Throughout Testing

Clean, dry sand has no cohesive strength. The addition of water to clean sand begins to increase the apparent cohesive strength, but only minimally due to capillary tension around points of contact between grains of sand. The addition of fines potentially increases the cohesive strength by filling in gaps within the sand matrix and allowing the fines to 'stick' to the sand and water more firmly. The increase of cohesive strength could be partially responsible for the diminishing PISCIS collection weights as FC was increased.

A study by Carraro et al. (2009) discussed the effects on sand shear strength and stiffness due to the addition of non-plastic fines that were nearly identical to the fines used in PISCIS tests. The authors suggested that the fines (silica flour) "interact with the irregularities on the surface of sand particles..." The interaction mentioned in the article was in reference to

the catching and interlocking of silica particles with the microscopic texture of the surface of sand granules. Although the sand used in the aforementioned study was round to sub-round, and the sand used in PISCIS testing was sub-angular, the interaction of fines with these sands would be very similar and more specifically related to the amount of pitting and surface weathering present on the sand particles. The catching and interlocking of fines with the sand particles would further increase the frictional strength of the test sand until there was enough fines present to dictate the test soil behavior. Increased frictional strength could also be partially responsible for the diminishing PISCIS collection weights as FC was increased. It should be noted that the aforementioned frictional strength increases to a threshold fines content at which point the fines begin to separate the sand particles from one another; when this happens, the frictional strength of the soil matrix is no longer primarily a product of the sand particles, but rather the fines that now exist between sand particles, which tends to decrease frictional strength.

5.2.2 Applied Overburden Pressure and Collected Sample Weight

The data displayed in Figure 5.2 indicate a minimal effect the overburden pressure applied to the test sand has on the sample weight collected. Before lab trials, the author postulated that additional overburden pressure in a frictional material would decrease the collected sample weight by increasing the shear strength of the test sand. This increase in shear strength would make the sand more resistant to the forces generated by the PISCIS. As higher load increments were tested, there was a noticeable jump in the resistance encountered when attempting to advance the dummy cone into the test sand which indicates that the sand was indeed gaining shear strength with increasing overburden pressures. However, this apparently only minimally affected the PISCIS collection weights.

The results in Figure 5.2 show an increase in mean collected sample weight of 18 grams as the applied overburden pressure increased for tests run at 0% fines content. For each fines content that followed (5, 10, 15, and 22%) the mean collected sample weights decreased as overburden increased. For 5% fines content, the mean decreased by 11 grams. The mean collected sample weight decreased similarly for 10, 15, and 22% fines by weights of 21, 23, and 24 grams respectively. It is my belief that, in clean sand, the increase in overburden

pressure created a scenario in which sand particles were more likely to 'pop' out of the hole wall when stimulated by the PISCIS, resulting in a slightly positive slope in Figure 5.2. Adding fines to the sand could have gradually enhanced the interlocking of sand particles when the overburden pressure was applied forcing the particles together and engaging particle contacts. While the shear strength of the sand-fines mixture was increasing with increased overburden pressure, the sample collection weights tended to decrease resulting in the negative slopes seen in Figure 5.2.

5.2.3 Implications of Results

As mentioned before, the current method for identifying caving hazards refers directly to the amount of fines present in the sand; this means that there is some point at which the test sand gains enough strength due to the addition of fines to resist caving forces and is no longer considered a drilling hazard. In addition to calibrating a functioning prototype, one of the goals of this thesis was to define the point at which the test sand undergoes this change. The results reveal that there is no specific fines content at which the test sand shifted behavior drastically, but rather, it was a gradual transformation. The drilling industry uses 15% as the FC that governs the sand's behavior, but the influence of fines can be seen in PISCIS tests at contents as low as 5 to 10%. This is not to say that the industry is incorrect in its assumptions, but simply that the influence of fines can be detected by the PISCIS well before the industry cutoff. If the results of PISCIS field tests can be correlated to CPT data taken from the test sites, a more accurate identification of caving hazards is theoretically possible.

CHAPTER 6: FUTURE RESEARCH AND CONCLUSIONS

6.1 Conclusions

After 13 prototype iterations, the Pneumatic In-Situ Soil Caving Index Sampler (PISCIS) was developed and calibrated under controlled lab conditions. During calibration testing, the fines content of the test sand was varied as well as the overburden pressure applied to the test sand. The results indicate that the PISCIS is capable of differentiating between a variety of fines contents based on the weight of collected samples. The relationship between fines content and collected sample weight is nearly exponential in nature with very high collection weights at 0% FC and low collection weights at 22% FC.

Within each fines content, the overburden pressure was increased from 36 to 218 KPa. This increase in overburden pressure caused an increase in collection weight at 0% FC. Then, as the FC was increased, the trend reversed, and increasing overburden pressure resulted in diminished collection weights. The effect of overburden pressure on PISCIS collection weight was minimal when compared to the effect of additional fines.

The knowledge gained from the design, development, lab testing, and analysis of the PISCIS has led to the belief that, after a few minor design adjustments, the prototype would be ready for field testing. With the field test results, an index could be generated that would help to identify drilled shaft caving hazards in sandy layers above the water table. Using this index, the drilling industry could save immense amounts of time, money (public and private), and fuel, simply by having a better understanding of what to expect when drilling.

6.2 Topics of Future Research

The PISCIS design, analysis, and calibration testing was conducted under very specific laboratory conditions. Even though the prototype functioned as intended, it is difficult to say with any certainty that it could continue to do so if the conditions were changed. The following sections outline some of the potential topics for future research that would supplement our understanding of the PISCIS results.

6.2.1 Test Sand

The specific type of sand encountered could have an impact on the PISCIS results. To understand the magnitude of this impact, lab tests could be run using sands with a variety of grain size distributions, particle shapes, and mineral contents (quartz, mica, etcetera). Knowing the effects of various sands could assist in the interpretation of PISCIS field tests, as no two sands encountered in the field will ever be alike.

6.2.2 Fines

As with sand, the specific type of fines the sand contains could impact the test results. Testing with high and low plasticity clays, plastic silt, and potentially organic fines would assist in the interpretation of PISCIS field tests.

6.2.3 Water Content

Lab tests were run on sand with gravimetric water contents ranging from 3 to 11%. The water contents were adjusted based on the amount of fines that were added to the mixture. Future testing could be conducted to determine the effects of varying the water content within a specific fines content. Also, tests could be prepared and left to sit for an extended period of time to determine what kind of yields could be expected from sand that is much drier than what could be properly “pluviated” without material segregation.

6.2.4 Triggering Mechanism

The interpretation of triggering mechanisms for lab prototypes remained macroscopic with regards to soil mechanics, but could certainly benefit from a more microscopic understanding of what takes place at the moment of triggering. Using a high speed camera, the initial burst of air from the PISCIS could be seen hitting the walls of the test hole and removing sand grains or clusters thereof. Understanding exactly how the PISCIS extracts samples can assist in interpretation and correlation of PISCIS tests and CPT results.

6.2.5 Air Pressure

Throughout the course of testing, the pneumatic pressure cell was filled to 100 psi. Lower pressures were used to test earlier prototypes, which led to the conclusion that higher test

yields were achieved with higher pressures. Further testing could be conducted at even higher pressures to determine if the relationships presented in this thesis remain constant, shift, or change entirely. This research would be most useful if the effects of the triggering mechanism were understood to be directly influenced by increased pressure.

6.2.6 Overconsolidation

All PISCIS testing was conducted under normally consolidated conditions. The same series of tests could be conducted after some of the pressure plates had been removed to determine if overconsolidation influences collection weights.

6.2.7 Field Trials

The scope of this thesis involved the calibration of the prototype but did not include field testing. For the results of PISCIS tests to have real world significance, field data must be collected, processed, and logged into a reference index. Additional data will be required to be able to say with any confidence whether or not the sand encountered in a soils report is likely to or unlikely to cave when drilling. Collecting these data points will constitute the bulk of future research.

BIBLIOGRAPHY

Belkhatir, Mostefa, Tom Schanz, and Ahmed Arab. “Effect of Fines Content and Void Ratio on the Saturated Hydraulic Conductivity and Undrained Shear Strength of Sand–silt Mixtures.” Environmental Earth Sciences 70.6 (2013): 2469-479. Web. 24 Apr. 2014.

Bell, J.S. “Practical Methods for Estimating in Situ Stresses for Borehole Stability Applications in Sedimentary Basins.” *Journal of Petroleum Science and Engineering* 38.3-4 (2003): 111-19. *ScienceDirect*. Web. 3 Mar. 2014.

Bell, J.S. “Sloughing of Cast in Drilled Hole Piles.” J*ournal of Petroleum Science and Engineering* 38.3-4 (2003): 111-19. Print.

Brown, D. A., John P. Turner, and Raymond J. Castelli. “4.2 Dry Method of Construction.” *Drilled Shafts: Construction Procedures and LRFD Design Methods*. McLean, VA: U.S. Dept. of Transportation, Federal Highway Administration, 2010. N. pag. Print.

Bower, Charlie. “Financial Implications of Caving Soil.” Personal interview. 9 April 2014. Project Manager for Case Pacific Co.

Carraro, J. Antonio H., Monica Prezzi, and Rodrigo Salgado. “Shear Strength and Stiffness of Sands Containing Plastic or Nonplastic Fines.” *Journal of Geotechnical and Geoenvironmental Engineering* 135.9 (2009): 1167-178. Print.

Caruso, Cary Wayne. “In Situ Measurement of the Scour Potential of Non-cohesive Sediments (ISEP).” Thesis. North Caroline State University, 2012. *NCSU Libraries*. 16 Aug. 2011. Web. 7 Mar. 2014.

Chakraborty, T., and R. Salgado. “Dilatancy and Shear Strength of Sand at Low Confining Pressures.” Journal of Geotechnical and Environmental Engineering (2010): 527-31. Web. 24 Apr. 20.

Chaney, R.C., K.R. Demars, A. Cresswell, M.E. Barton, and R. Brown. “Determining the Maximum Density of Sands by Pluviation.” *Geotechnical Testing Journal* 22.4 (1999): 324. Print.

Coduto, Donald P. *Foundation Design: Principles and Practices*. 2nd ed. Upper Saddle River, NJ: Prentice Hall, 2001. Print.

De Ruiter, J. “Current Penetrometer Practice.” *Cone Penetration Testing and Experience: Proceedings of a Session Sponsored by the Geotechnical Engineering Division at the ASCE National Convention, St. Louis, Missouri, October 26-30, 1981*. Ed. G. M. Norris and R. D. Holtz. New York: ASCE, 1981. 32-33. Print.

Douglas, Bruce J., and Richard S. Olsen. “Soil Classification Using Electric Cone Penetrometer.” *Cone Penetration Testing and Experience: Proceedings of a Session Sponsored by the Geotechnical Engineering Division at the ASCE National Convention, St. Louis, Missouri, October 26-30, 1981*. Ed. G. M. Norris and R. D. Holtz. New York: ASCE, 1981. 209-15. Print.

Gavin, K. G., D. Cadogan, and P. Casey. “Shaft Capacity of Continuous Flight Auger Piles in Sand.” *Journal of Geotechnical and Geoenvironmental Engineering* 135.6 (2009): 790-98. *ASCE Library*. 18 Feb. 2009. Web. 21 Sept. 2012.

Holtz, R. D., and William D. Kovacs. *An Introduction to Geotechnical Engineering*. 2nd ed. Englewood Cliffs, NJ: Prentice-Hall, 2011. Print.

Igwe, Ogbonnaya, Hiroshi Fukuoka, and Kyoji Sassa. “The Effect of Relative Density and Confining Stress on Shear Properties of Sands with Varying Grading.” Geotechnical and Geological Engineering 30.5 (2012): 1207-229. Web. 24 Apr. 2014.

Judd, Dave. “Determination of Drilling Industry Standards of Practice.” Telephone interview. 21 Sept. 2012. Chief Estimator for Case Pacific Co.

Kim, Kyoung-Yul, Dae-Soo Lee, Jaeyeon Cho, Sang-Seom Jeong, and Sungjune Lee. “The Effect of Arching Pressure on a Vertical Circular Shaft.” Tunnelling and Underground Space Technology 37 (2013): 10-21. Web. 24 Apr. 2014.

Lee, Junhwan, Doohyun Kyung, Jungmoo Hong, Feng Zhang, and Ke Yang. “Estimation of In-situ Strength for Sandy Soils Using CPT Cone Resistance.” *Deep Foundations and Geotechnical In Situ Testing*. Proc. of GeoShanghai International Conference, Shanghai, China. Ed. Robert Y. Liang. New York: ASCE, 2010. 361-67. Print.

Lee, Junhwan, Rodrigo Salgado, and J. Antonio H Carraro. “Stiffness Degradation and Shear Strength of Silty Sands.” *Canadian Geotechnical Journal* 41.5 (2004): 831-43. Print.

Liu, Cheng, and Jack B. Evett. *Soils and Foundations*. 7th ed. Englewood Cliffs, NJ: Prentice-Hall, 2008. Print.

Lu, Ning, Bailin Wu, and Chee P. Tan. “Tensile Strength Characteristics of Unsaturated Sands.” Journal of Geotechnical and Geoenvironmental Engineering 133.2 (2007): 144-54. Web. 24 Apr. 2014.

Lunne, Tom, and Arne Kleven. “Role of CPT in North Sea Foundation Engineering.” *Cone Penetration Testing and Experience: Proceedings of a Session Sponsored by the Geotechnical Engineering Division at the ASCE National Convention, St. Louis, Missouri, October 26-30, 1981*. Ed. G. M. Norris and R. D. Holtz. New York: ASCE, 1981. 86-91. Print.

Lunne, Tom, Peter Kay Robertson, and John J. M. Powell. *Cone Penetration Testing in Geotechnical Practice*. London: Blackie Academic & Professional, 1997. Print.

Mitchell, James K., and Tom A. Lunne. “Cone Resistance as a Measure of Sand Strength.” *Journal of the Geotechnical Engineering Devision* 104.GT7 (1978): 995-1001. Print.

Muromachi, Tadahiko. “Cone Penetration Testing in Japan.” *Cone Penetration Testing and Experience: Proceedings of a Session Sponsored by the Geotechnical Engineering Division at the ASCE National Convention, St. Louis, Missouri, October 26-30, 1981*. Ed. G. M. Norris and R. D. Holtz. New York: ASCE, 1981. 52-57. Print.

Pardo, G. S., and E. Saez. “Experimental and Numerical Study of Arching Soil Effect in Course Sand.” Computers and Geotechnics 57 (2014): 75-84. Web. 24 Apr. 2014.

Rohani, Behzad, and George Y. Baladi. “Correlation of Cone Index with Soil Properties.” *Cone Penetration Testing and Experience: Proceedings of a Session Sponsored by the Geotechnical Engineering Division at the ASCE National Convention, St. Louis, Missouri, October 26-30, 1981*. Ed. G. M. Norris and R. D. Holtz. New York: ASCE, 1981. 128-43. Print.

Salgado, R., and M. Prezzi. “Computation of Cavity Expansion Pressure and Penetration Resistance in Sands.” *International Journal of Geomechanics* 7.4 (2007): 251-65. Print.

Salgado, R., P. Bandini, and A. Karim. “Shear Strength and Stiffness of Silty Sand.” Journal of Geotechnical and Geoenvironmental Engineering 126.5 (2000): 451-62. Web. 24 Apr. 2014.

Salgado, Rodrigo. *The Engineering of Foundations.* Boston: McGraw Hill, 2008. Print.

Sánchez, Francisco, and Mansoor H. Al-Harthy. “Risk Analysis: Casing-while-Drilling (CwD) and Modeling Approach.” *Journal of Petroleum Science and Engineering* 78.1 (2011): 1-5. *ScienceDirect*. Web. 3 Mar. 2014.

Sowers, George F. *Introductory Soil Mechanics and Foundations: Geotechnical Engineering*. 4th ed. New York: Macmillan, 1979. Print.

Tobar, Tatiana and Mohamed A. Meguid. “Comparative Evaluation of Methods to Determine the Earth Pressure Distribution on Cylindrical Shafts: A Review.” Tunnelling and Underground Space Technology 25 (2010): 188-97. Web. 24 Apr. 2014.

United States. Army. Corps of Engineers. *Engineering and Design: Bearing Capacity of Soils*. Washington: Govt. Print. Off., 1992. Print. E.M. 1110-1-1905.

Wang, X., and R.I. Sterling. “Stability Analysis of a Borehole Wall during Horizontal Directional Drilling.” *Tunnelling and Underground Space Technology* 22.5-6 (2007): 620-32. *ScienceDirect*. Web. 3 Mar. 2014.

Wu, Chao, Mian Chen, and Yan Jin. “Real-time Prediction Method of Borehole Stability.” *Petroleum Exploration and Development* 35.1 (2008): 80-84. *ScienceDirect*. Web. 3 Mar. 2014.

Yang, J. “Influence Zone for End Bearing of Piles in Sand.” *Journal of Geotechnical and Geoenvironmental Engineering* 132.9 (2006): 1229. *EBSCO - Academic Search Premier*. Web. 21 Sept. 2012.

Yang, Z. X., R. J. Jardine, B. T. Zhu, and S. Rimoy. “Stresses Developed around Displacement Piles Penetration in Sand.” J*ournal of Geotechnical and Geoenvironmental Engineering* (2013): 04013027. Print.

Zornberg, Jorge G., Nicholas Sitar, and James K. Mitchell. “Limit Equilibrium as Basis for Design of Geosynthetic Reinforced Slopes.” *Journal of Geotechnical and Geoenvironmental Engineering* 124.8 (1998): 684. Print.

APPENDICES

APPENDIX A: PROTOTYPE DESIGN AND DEVELOPMENT

Contained herein is a journalistic documentation of each of the nine prototypes, an analysis of their lab performances, and projections for future development, as they took place in real time.

A.1 Prototype 1

A.1.1 Description

Prototype 1 (see Figure A.1) is an eight-prong mechanical triggering device (two flights of four prongs) constructed out of a 3/4” steel pipe. 1/8” rod is used as a pivoting pin for each prong and welded into grooves that are machined into the 3/4” pipe nipple. Electrical pulls are repurposed to function as the triggering prongs. A steel rod pushed downward within the pipe will force the prongs into the open position, thereby agitating the walls of the test hole.

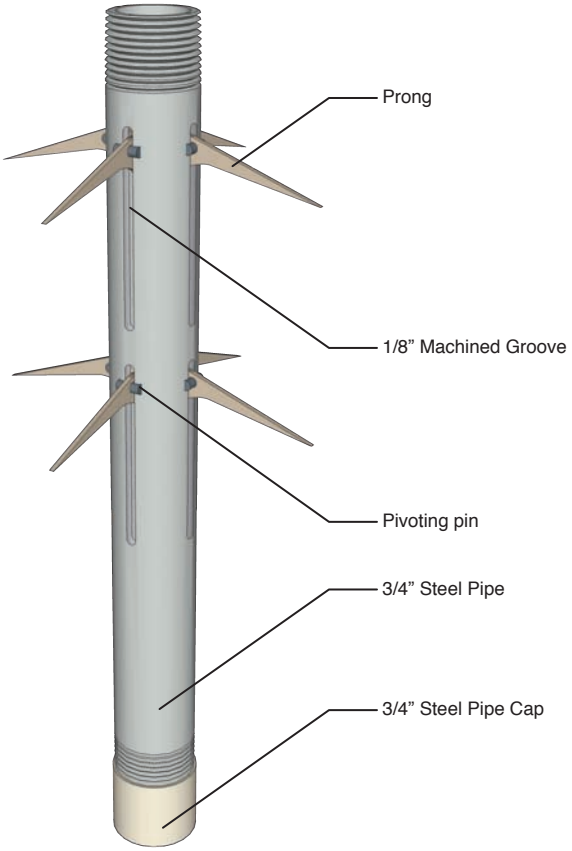

FIGURE A.1: Prototype 1

A.1.2 Design Analysis

- The overall design was too large to fit down a 1.400” diameter test hole with sufficient room to allow the disturbed sand to fall freely around the prototype and into a collection vessel below.
- Welding the pivoting pins in place pulled the triggering prongs out of alignment when the weld metal cooled (See Figure A.2).
- The steel rod that would force the prongs into the open position must fit the inside diameter of the prototype very closely to guarantee that all prongs are pushed open equally (see Figure A.3).

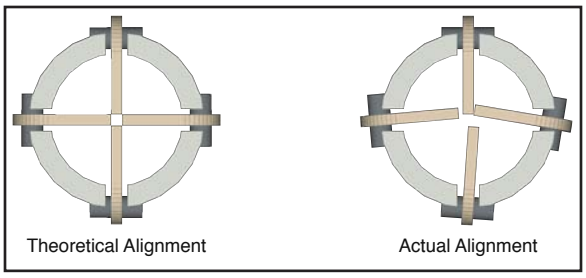

FIGURE A.2: Prong Alignment

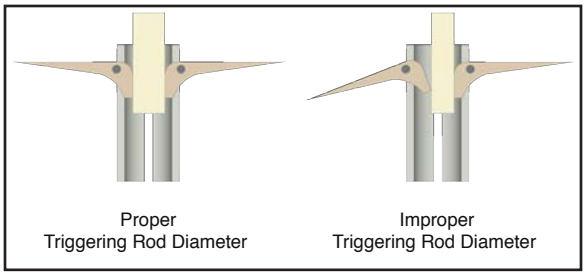

FIGURE A.3: Triggering Rod Diameter

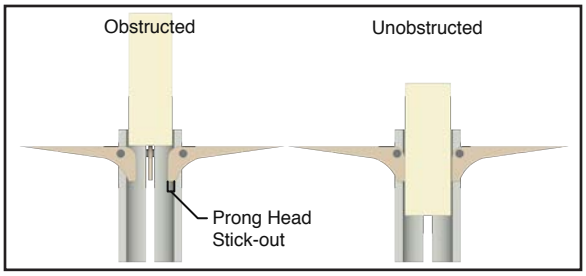

FIGURE A.4: Prong Placement

A.1.3 Projected Adjustments

- The next prototype must be more slender to allow for free downward movement of the disturbed test sand.
- Triggering prongs should be machined to ensure a more consistent position of the pivoting pin hole and to maximize their length.
- The pivoting pins should be welded into the wall thickness of the pipe to reduce the stick-out of prongs in the closed position beyond the face of the pipe.
- The distance from the top of the prong to the pivot pin must be adjusted or controlled so that when the prongs are in the open position, the top of the prong is coincident with the interior wall of the pipe to allow the triggering rod to pass through the device unobstructed (see Figure A.4).

A.2 Prototype 2

A.2.1 Description

Prototype 2 (see Figure A.5) is an eight-prong (two flights of four prongs) mechanical triggering device constructed out of a 1/2” steel pipe. 1/16” piano wire is used as a pivoting pin and is welded into grooves machined into the 1/2” pipe. Light gauge (approximately 1/16” thick) sheet steel is used for the prongs. A steel rod pushed downward within the pipe will force the prongs into the open position.

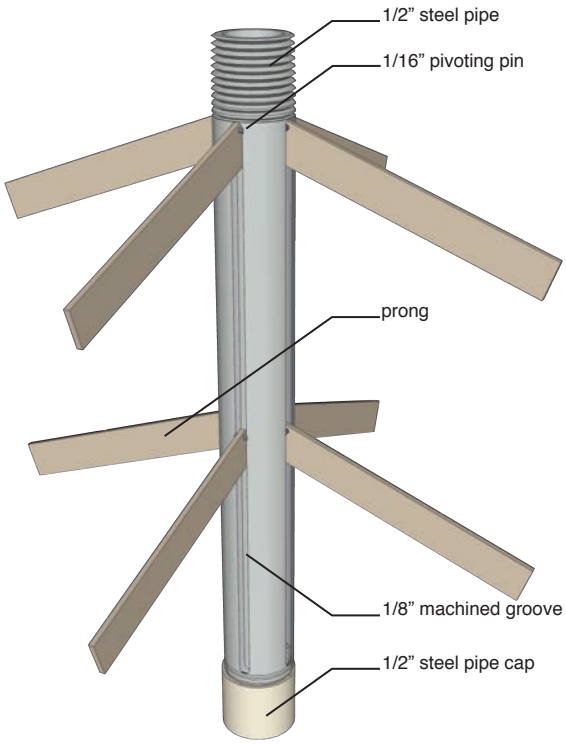

FIGURE A.5: Prototype 2

A.2.2 Design Analysis

- Four continuous longitudinal grooves were machined into the 1/2” pipe (rather than eight individual grooves as in the previous prototype). Then, horizontal grooves were cut to allow the pin connections to be welded into the wall thickness of the pipe. Machining the pipe in this way weakened it and made it difficult to clamp and machine. Upon welding the first pin connections into the grooves, the flimsy nature of the machined pipe exacerbated heat induced expansion and formed a kink in the middle of the pipe that could not be forced back into place.

- Due to the highly hardened nature of the piano wire used as a pivoting pin, there was difficulty welding the pins into the grooves of the mild steel pipe.

- The triggering prongs were still slightly out of alignment after welding the pivoting pins to the pipe, but there was a noticeable improvement relative to the previous prototype.

• The triggering prongs were adjusted to sit flush with the outside of the pipe in the closed position and flush with the inside of the pipe in the open position to minimize the prototype profile and ensure equal prong extension when triggered respectively (see Figure A.6).

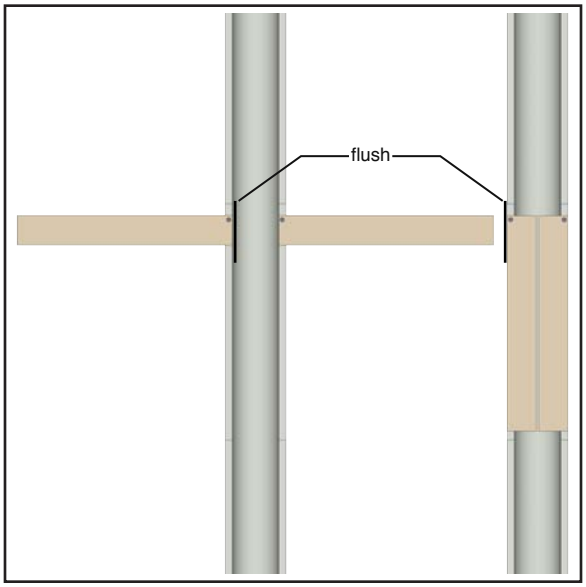

FIGURE A.6: Prongs in Flush Position

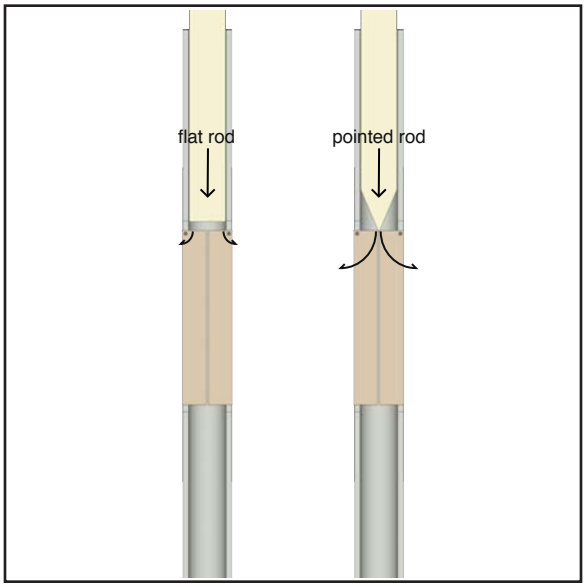

FIGURE A.7: Triggering Rod/Prong Interaction

• Attempting to trigger the prototype caused the prongs to either sheer off at the top or break the pivoting pin at the welded connection; This was due to the triggering rod generating a large sheer force rather than a rotational force in the prongs.

A.2.3 Projected Adjustments

• Both the prongs and the pivoting pins should be sized up to withstand the forces associated with triggering.

• The triggering rod must be machined to apply downward force to the inner-most edge of the triggering prongs to generate a larger rotational force that would open the prototype more effectively (see Figure A.7).

A.3 Prototype 3

A.3.1 Description

Prototype 3 (see Figure A.8) is a two-prong (two flights of one prong each) mechanical triggering device constructed out of a 1/2” steel pipe. 1/8” steel rod is used as a pivoting pin and is welded into grooves machined into the 1/2” pipe. 1/8” x 3/4” x 4” steel bar is used for the triggering prongs. A steel triggering rod with a machined tip

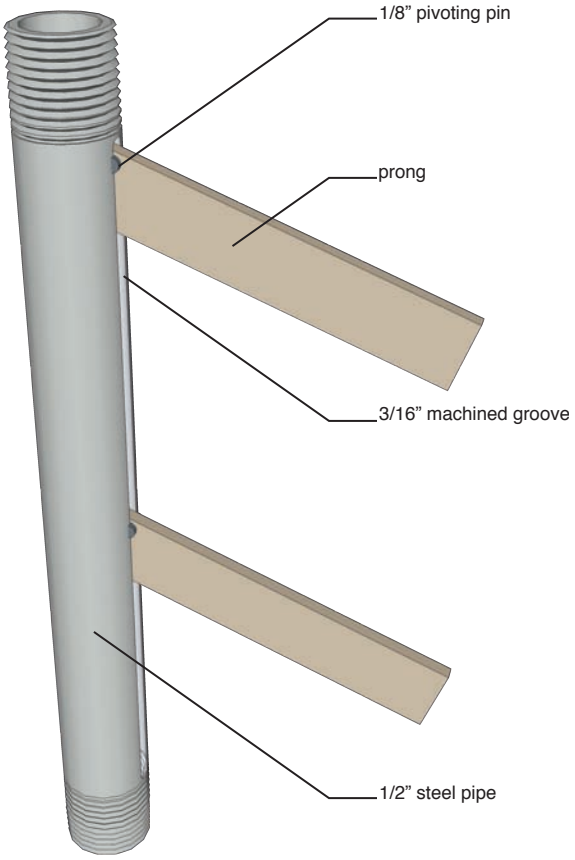

FIGURE A.8: Prototype 3

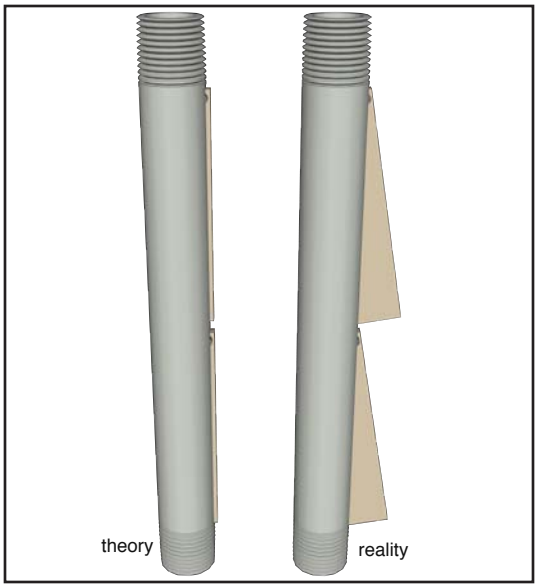

FIGURE A.9: Prong At-Rest Position

would, again, be used to force the prongs into the open position.

A.3.2 Design Analysis

- A singular 3/16” longitudinal groove was cut into the pipe which eliminated the occurrence of heat induced deformation upon welding the prongs and pivoting rod in place.
- The prongs opened evenly when triggered due to increased accuracy in positioning the pivot pins.
- The thicker prongs and pivot pins were able to resist the force of triggering without breaking or shearing off.
- Because each flight had only one prong, more rotational force could be applied to the prongs. Unfortunately, this design resulted in an intrinsic balancing problem in the at-rest position of the prongs and the device would not fit down the test hole (see Figure A.9).

• In hindsight, the asymmetric nature of the design would generate an unbalanced force when triggering the device underground. It would be difficult to guarantee the repeatability of the tests and would generate an unwanted source of sample variation.

A.3.3 Projected Adjustments

• Achieve the same strength and accuracy of Prototype 3 but with a symmetric design.

A.4 Prototype 4

A.4.1 Description

Prototype 4 (see Figure A.10) is a four-prong (two flights of two prongs) mechanical triggering device constructed out of a 1/2" steel pipe. 1/8" x 1/2" x 4" steel bar is used for the prongs and 1/8" rod is used for the pivoting pins. The prongs and pins are welded into two longitudinal groves cut in each side of the pipe. A steel rod with a machined tip is pushed downward within the pipe in a specific orientation to force the prongs into the open position.

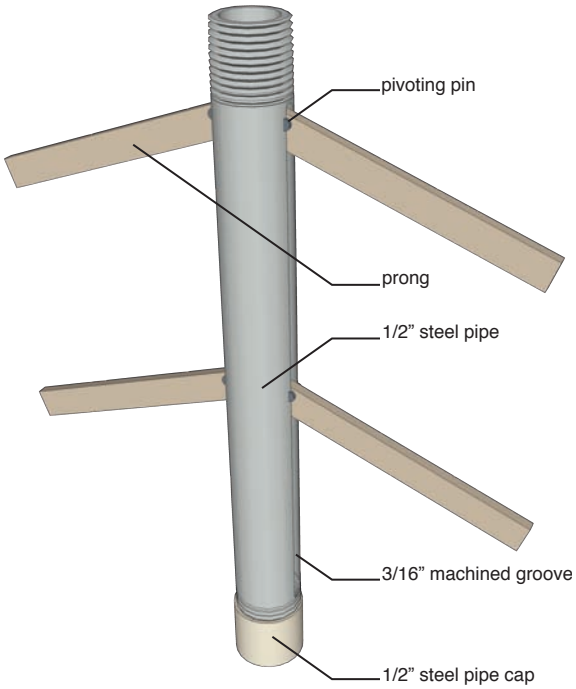

FIGURE A.10: Prototype 4

A.4.2 Design Analysis

• Great care was taken when welding the pivoting pins in place, which ensured the proper alignment of each flight of prongs.

• The triggering rod was machined to a thickness that guaranteed the prongs would open fully and evenly, thereby addressing a shortcoming of previous symmetric prototypes.

• The triggering prongs were shortened to make it possible to manually open the device while in the test hole.

• Although the prototype functioned properly, it yielded very little disturbed test sand in initial lab trials. Attempts to rotate

the prototype within the hole while in the open position collected larger sample volumes, but proved to be difficult to control and inconsistent from one trial to another.

- Although the prototype could be triggered manually, the speed at which the prongs would open was highly variable and therefore became a source of inconsistency between tests. This issue must be addressed. Repeatability is paramount in calibrating a functioning prototype.
- The ability of vertically oriented prongs to disturb the hole walls was called into question after running the tests. Perhaps a horizontally oriented prong would generate a scenario where the hole walls are more likely to fail.

A.4.3 Projected Adjustments

- Create a horizontally oriented mechanical triggering prototype.
- Consider rotating said horizontally-oriented prototype to affect the entire hole perimeter.
- Generate a design where the triggering process is smooth, controlled, and repeatable.
- Consider other forms of triggering as an alternative (not mechanical).

A.4.4 Catchment Evolution

A section of steel tube must sit below the aforementioned prototypes to catch the sand dislodged during testing. The following Sections are a description of the catchment design and evolution that took place simultaneously with the design of Prototype 4.

A.4.5 Prototype 4.1

A.4.5.1 Description

Prototype 4.1 (see Figure A.11) is a 1-5/16” thin walled steel pipe that is 8 inches long and closed at one end. 1/8” rod is welded to the upper edge of the open side and then to a 1/2” pipe cap that threaded into the bottom of Prototype 4.

A.4.5.2 Design Analysis

- The shrinkage caused by welding the thin metal elements made it extremely difficult to center the pipe cap during fabrication. The result was a rigid catchment attachment

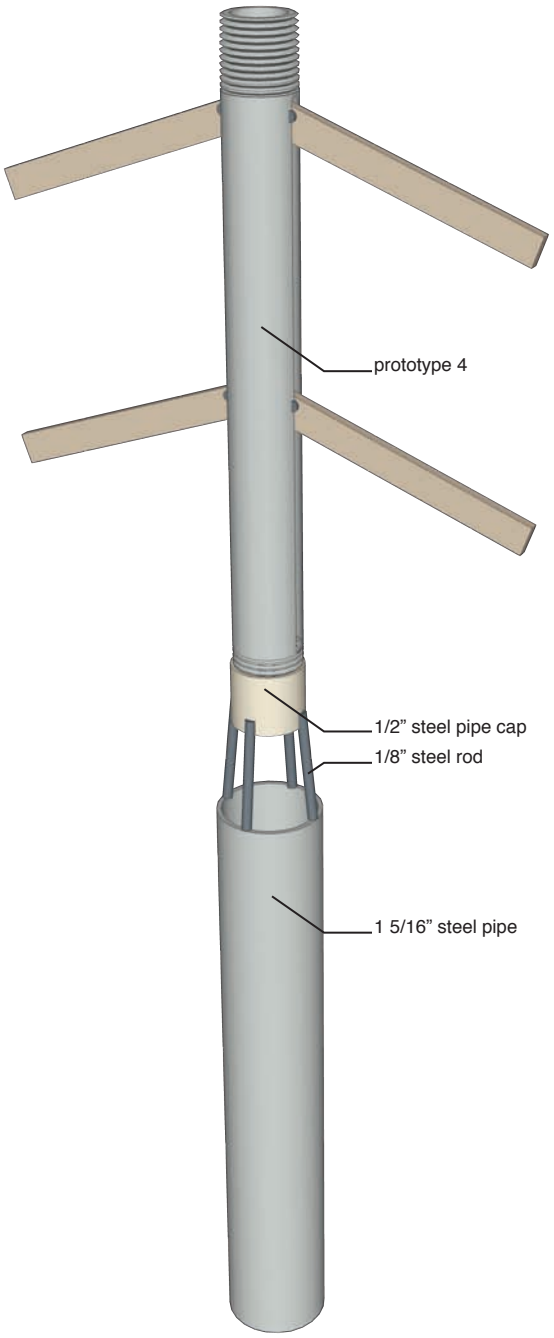

FIGURE A.11: Prototype 4.1

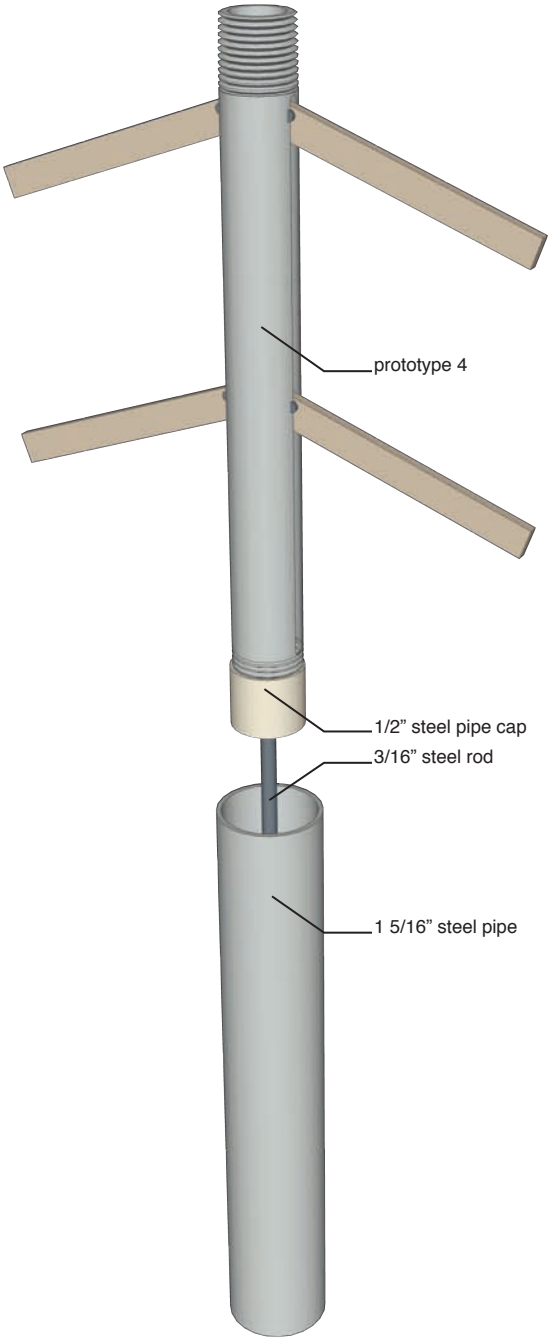

FIGURE A.12: Prototype 4.2

that was not aligned properly with Prototype 4. This made it impossible to advance the prototype into the test hole without affecting the hole walls before the test took place.

A.4.5.3 Projected Adjustments

- Generate a catchment prototype that will axially align with Prototype 4.

A.4.6 Prototype 4.2

A.4.6.1 Description

Prototype 4.2 (see Figure A.12) is a 1-5/16” thin walled steep pipe, 8 inches long and closed at one end. A 3/16” steel rod is threaded into the center of the closed end (bottom) of the catchment tube. A hole is drilled in the center of a 1/2” pipe cap and the steel rod is pushed into this hole and welded in place. This assembly is then threaded into the bottom of Prototype 4.

A.4.6.2 Design Analysis

- The design ensured the proper axial alignment of the catchment tube and Prototype 4 and was flexible enough to make minor adjustments.

- Collected test samples could be easily retrieved simply by un-threading the catchment tube from the connection rod.

- In an attempt to minimize the profile of the catchment system, the walls of the 1/2” pipe cap were sanded down. Although this allowed sand to fall into the catchment tube unobstructed, it also reduced the strength of the pipe cap significantly. During lab trials, the triggering rod used to open Prototype 4 hit the pipe cap and broke through (see Figure A.13).

A.4.6.3 Projected Adjustments

- Generate a catchment prototype that can withstand the force of the triggering rod while also being low profile and remaining axially aligned with Prototype 4.

FIGURE A.13: Triggering Rod Blowout

A.4.7 Prototype 4.3

A.4.7.1 Description

Prototype 4.3 (see Figure A.14) is the steel tube and connection rod from Prototype 4.2 with a new interface piece welded to Prototype 4. 3/16” grooves are cut into the bottom of Prototype 4 and a setscrew assembly is pushed into the bottom of the 1/2” pipe. The setscrew assembly is welded into the bottom of Prototype 4. The connection rod is then pushed up through the middle of the setscrew assembly and the screw is tightened.

A.4.7.2 Design Analysis

- The design was very strong and easily resisted the force of the triggering rod.
- It was difficult to maintain axial alignment because the entire catchment system was attached with only one point of contact (the setscrew). The catchment tube was able to pivot slightly and sat off axis when the screw was fully tightened.

A.4.7.3 Projected Adjustments

- Create an adjustable connection so that Prototype 4 and the catchment tube can be properly aligned.

A.4.8 Prototype 4.4

A.4.8.1 Description

Prototype 4.4 (see Figure A.15) is the steel tube and connection rod from Prototype 4.3 with a new interface piece welded to prototype 4. A 1-inch long 1/2” steel rod is center drilled to fit the 3/16” connection rod. Three holes are drilled along the length of the piece, each hole oriented 120 degrees away from the last. The holes are threaded and setscrews are placed in each of them. The piece is welded to the bottom of Prototype 4 after the last catchment iteration is removed. The connection rod is then pushed up into the center hole and the setscrews are tightened.

A.4.8.2 Design Analysis

- The design held the catchment system firmly in position below Prototype 4 while also allowing for fine adjustment of orientation.

A.4.8.3 Projected Adjustments

- Attach the catchment system to future prototypes as needed.

A.5 Prototype 5

A.5.1 Description

Prototype 5 (see Figure A.16) is a two-prong (two flights of one prong each) mechanical triggering device constructed from thick-walled drawn-over-mandril (DOM) pipe. Two slices of the DOM pipe are cut in half and welded to 1/8” pivoting rods to act as the triggering prongs. A steel rod is machined to fit within the DOM pipe and two small keys are welded to the rod to be able to push open the prongs when the rod is rotated clockwise. An exploded view can be seen in Figure A.17 demonstrating how the prototype functions. The catchment system from Prototype 4.4 is welded to Prototype 5.

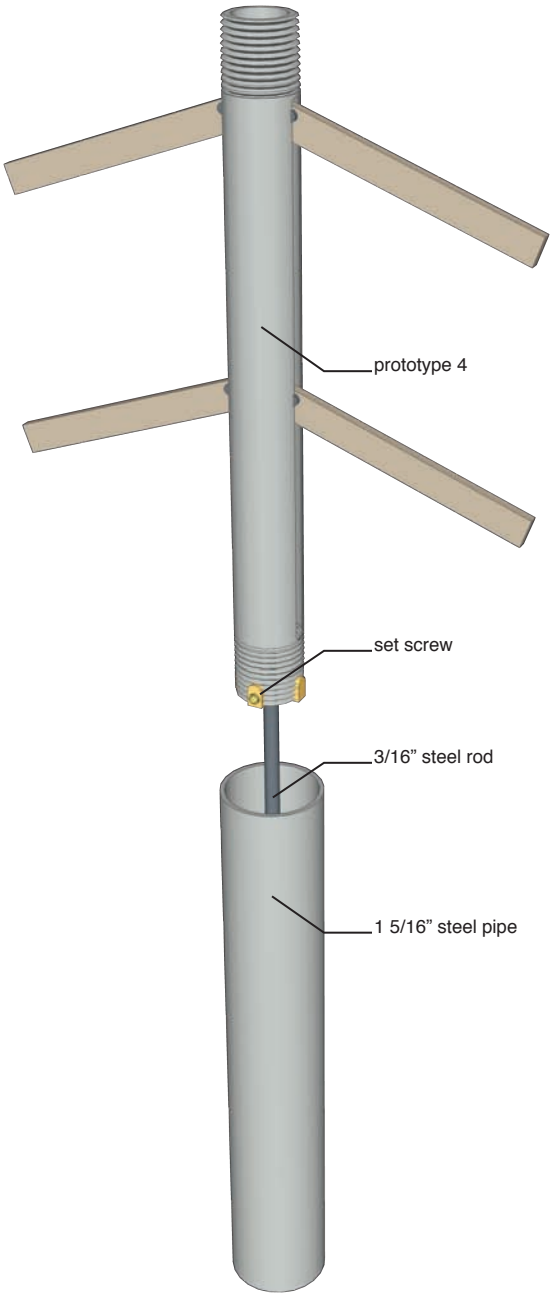

FIGURE A.14: Prototype 4.3

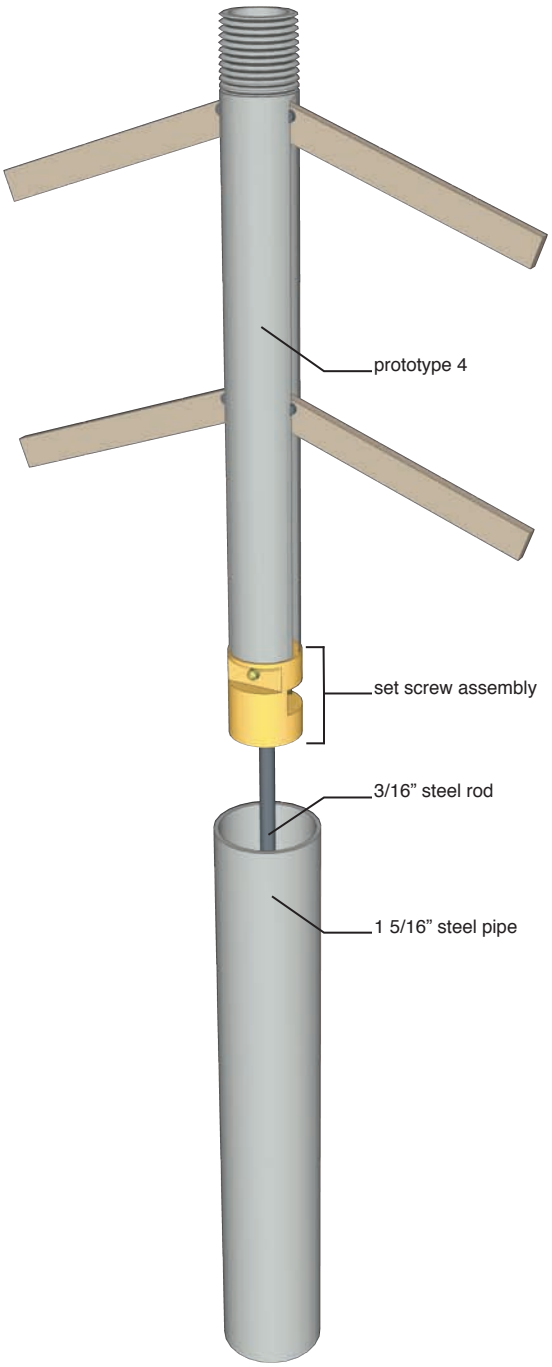

FIGURE A.15: Prototype 4.4

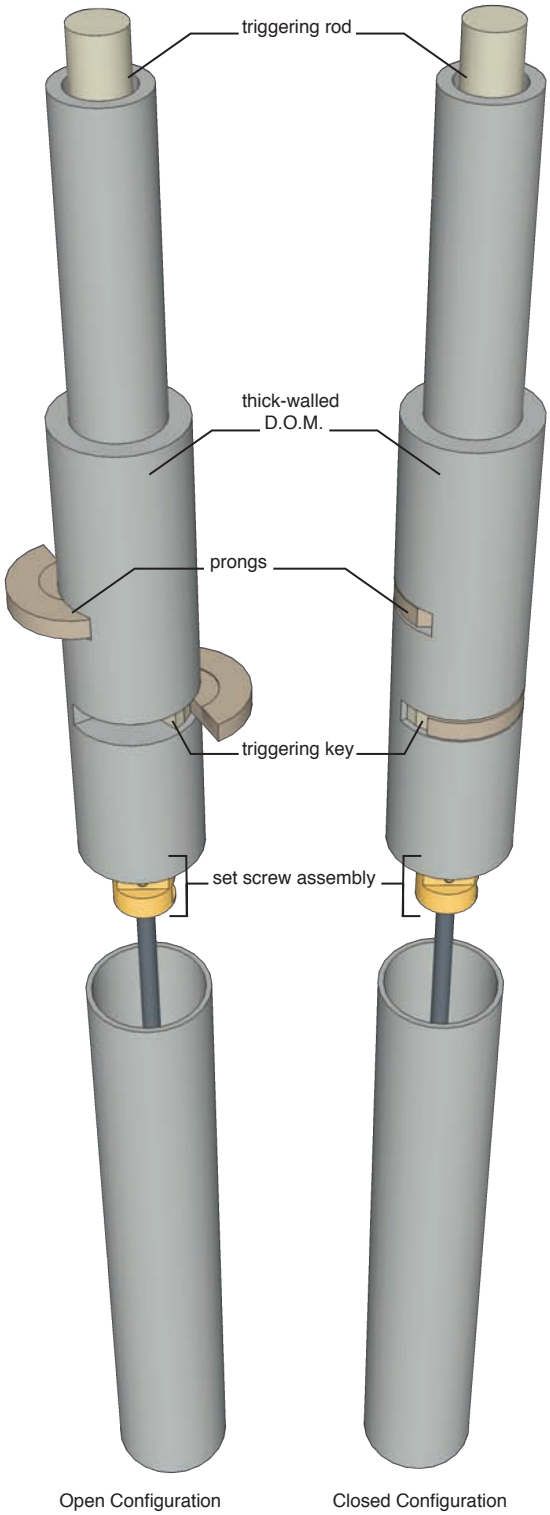

FIGURE A.16: Prototype 5

A.5.2 Design Analysis

- The prongs extended evenly and maintained the central orientation of the prototype within the hole.
- No supporting equipment was constructed to maintain the central position of the prototype within the hole during rotation. Should the prototype function favorably, this issue should be addressed.
- The triggering process was smooth, and controlled. When Prototype 5 was rotated in the test hole, it generated two parallel indentations in the hole wall as anticipated.
- Despite the design functioning as it was intended mechanically, the collected yield was insufficiently small and, unfortunately, the design does not allow for adjustments of any kind.

A.5.3 Projected Adjustments

- Design and construct a pneumatic triggering device that is easily adjusted/ retrofitted to make minor changes.
- Construct a pressure cell of a given volume that consistently releases pressurized air and can display internal pressure for data collection purposes.

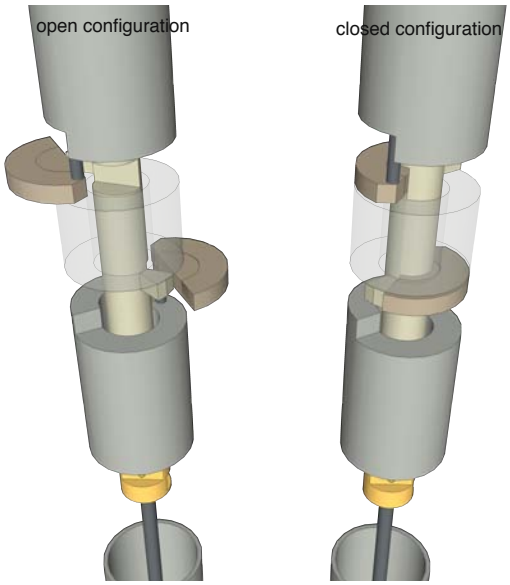

FIGURE A.17: Exploded View of Prototype 5

A.6 Prototype 6a

A.6.1 Description

Prototype 6a (see Figure A.18) is a pneumatic triggering device attached to the end of a 3/8” steel rod. A steel manifold is welded to the end of the rod to receive four 1/8” air hoses (via threaded pressure connections) and direct those hoses out of the bottom of the manifold into four 1/8” by 7-inch long capped pipes that act as pneumatic distribution nozzles. Three slits are cut into each pipe at one inch spacing for a total of 12 air distribution slits. A 2” diameter x 5 foot long PVC pipe is capped at one end and fitted with a threaded reducer at the other. The pipe is reduced to 1/4” brass pipe along which a pressure gauge, a tire valve, and a ball valve are attached. Beyond the ball valve, the 1/4” pipe is split into 1/8” threaded ports to receive the four air hoses that connect to the manifold. The catchment system from Prototype 4.4 is adjusted to reach the bottom of the manifold where it is held with a setscrew. An inflatable latex bubble is positioned at the mouth of the catchment tube and is inflated after the test was run to seal off the tube and preserve the sample as the prototype is extracted from the test hole.

A.6.2 Design Analysis

- When tested at the maximum pressure attainable (100psi), the collected yield was greater than Prototypes 4 and 5 but still insufficiently small.
- The collected yield across separate tests was fairly consistent (1.1 to 1.4 oz. collected) which indicated that further design iterations could prove fruitful.
- Disturbed test sand was moving upwards with the flow of air and becoming lodged on and around the manifold. The sand would fall into the catchment tube in some trials and not in others. This was a source of variation that had to be addressed.

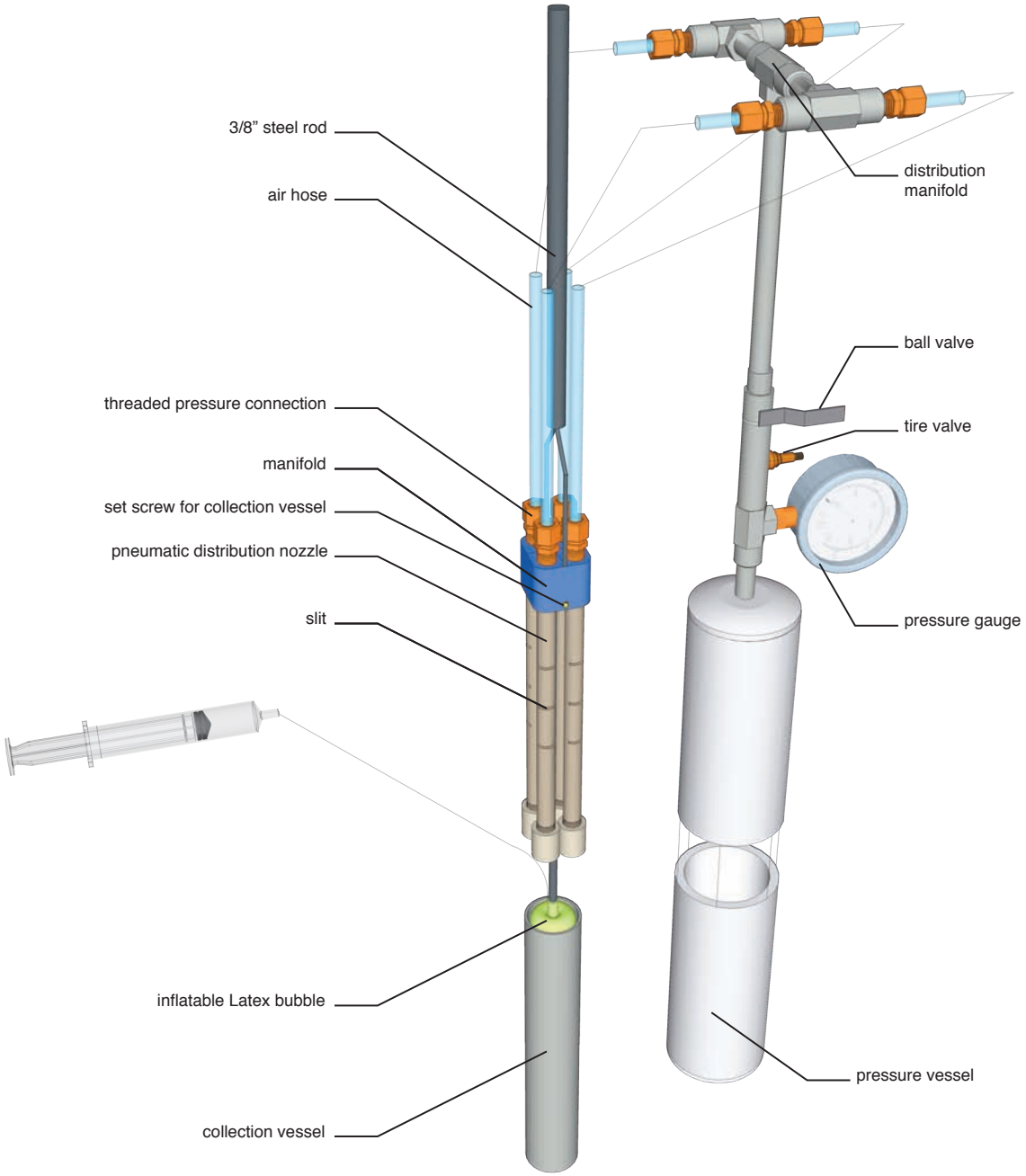

FIGURE A.18: Prototype 6a

A.6.3 Projected Adjustments

- Reduce the number of slits in the pneumatic distribution nozzles to concentrate air-flow in an attempt to collect greater yields. Perhaps the decrease in slits will also reduce the amount of sample that gets lodged on and around the manifold.

A.7 Prototype 6b

A.7.1 Description

Prototype 6b (see Figure A.19) is Prototype 6a with the four 7-inch long pneumatic distribution nozzles switched out for four 3-inch long pneumatic nozzles. Each new nozzle has only two slits for a total of eight.

A.7.2 Design Analysis

- As postulated, the collected yield was higher (1.8 to 2.4 oz.) than Prototype 6a.
- The disturbed test sand was still becoming lodged on and around the manifold.
- The prototype was able to collect enough sample to fill the catchment tube, but there was still significant variation between tests.

A.7.3 Projected Adjustments

- Attempt to reduce the flow rate of air into the test hole by further reducing the number of pneumatic distribution slits, which will subsequently concentrate the air streams for greater yields.
- Remove two pneumatic distribution nozzles and replace them with threaded 1/8” plugs.
- Add a quick release pressure coupling between the prototype and the pressure vessel to increase testing efficiency.

A.8 Prototype 6c

A.8.1 Description

Prototype 6c (see Figure A.20) is Prototype 6b with two of the four pneumatic distribution nozzles removed and replaced with threaded plugs, resulting in two nozzles with two slits each for a total of four slits. A quick release connection is added to increase ease of testing.

A.8.2 Design Analysis

- The amount of variation between trials decreased, but was still too variable.

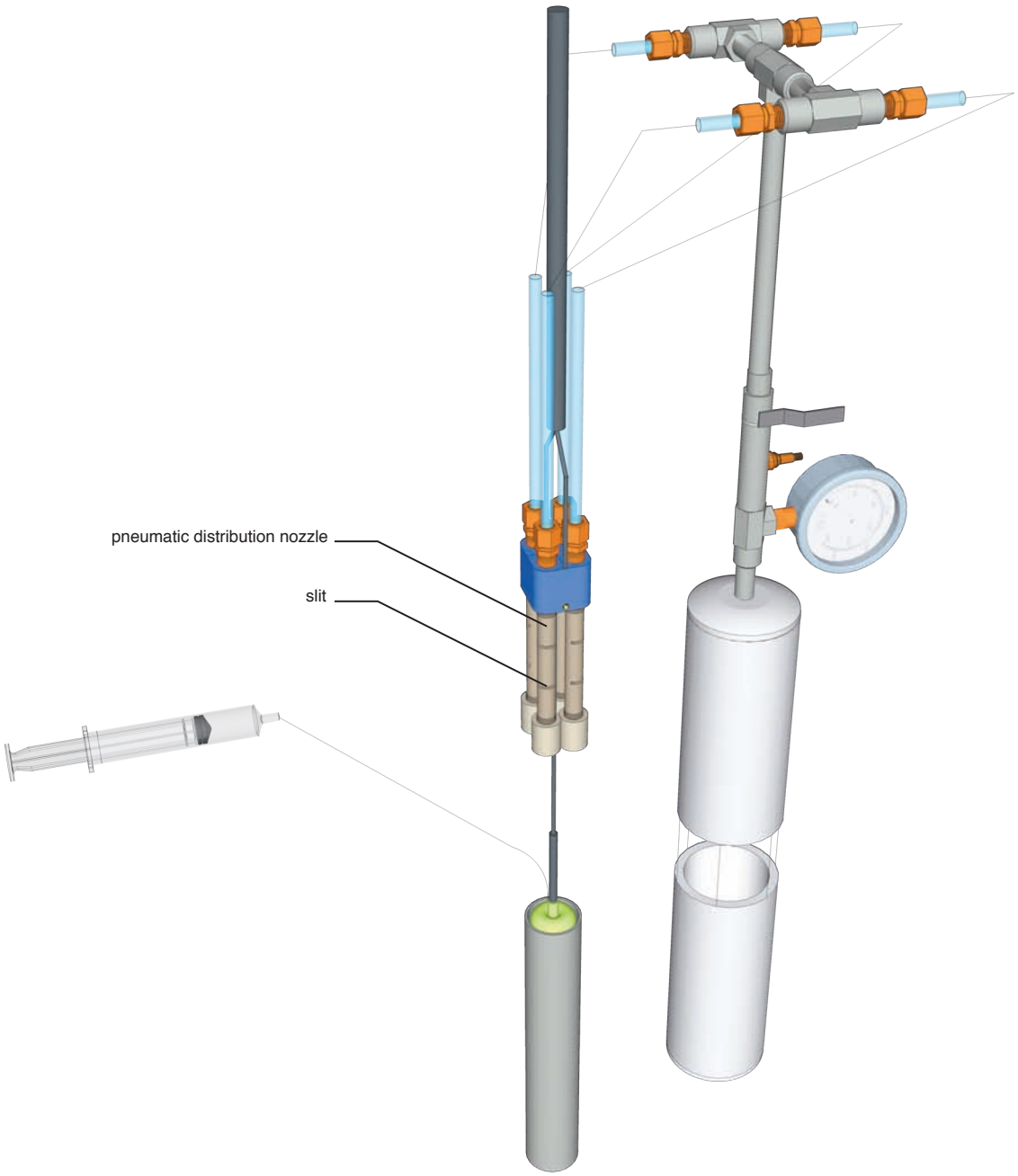

FIGURE A.19: Prototype 6b

- Disturbed sand still became lodged on and around the manifold and contributed to trial variation.

A.8.3 Projected Adjustments

- Further reduce the number of pneumatic distribution slits to see if this will decrease the variation in results.

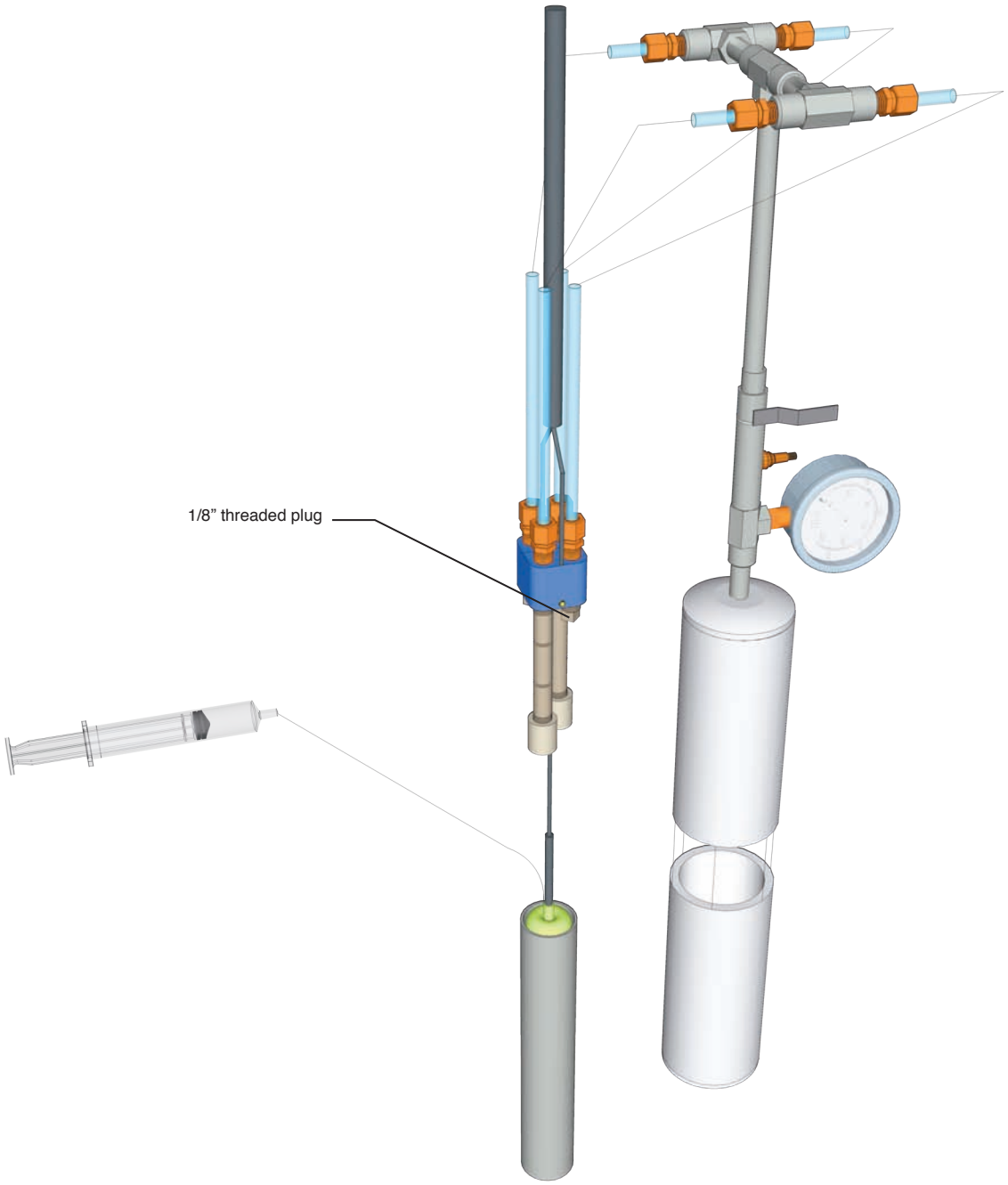

FIGURE A.20: Prototype 6c

A.9 Prototype 6d

A.9.1 Description

Prototype 6d (see Figure A.21) is Prototype 6c with only two pneumatic distribution slits rather than four.

A.9.2 Design Analysis

- Collected yields were higher than previous prototypes, but the same level of variation between tests remained.
- Disturbed test sand was still becoming lodged on and around the manifold.

A.9.3 Projected Adjustments

- Redesign the air distribution block/manifold to be smaller in an attempt to allow disturbed sand to more easily fall down around the device and into the catchment tube.
- A hanging catchment tube should be considered to address problems keeping the tube centered and vertical within the test hole.
- A larger collection tube (both diameter and length) should be used to reduce the annulus around the tube into which disturbed test sand was being lost.
- The pressure cell should be enlarged to increase the amount of pressurized air released during the test.
- A larger diameter air hose will be used to generate a stronger impulse of air to collect a larger sample size.

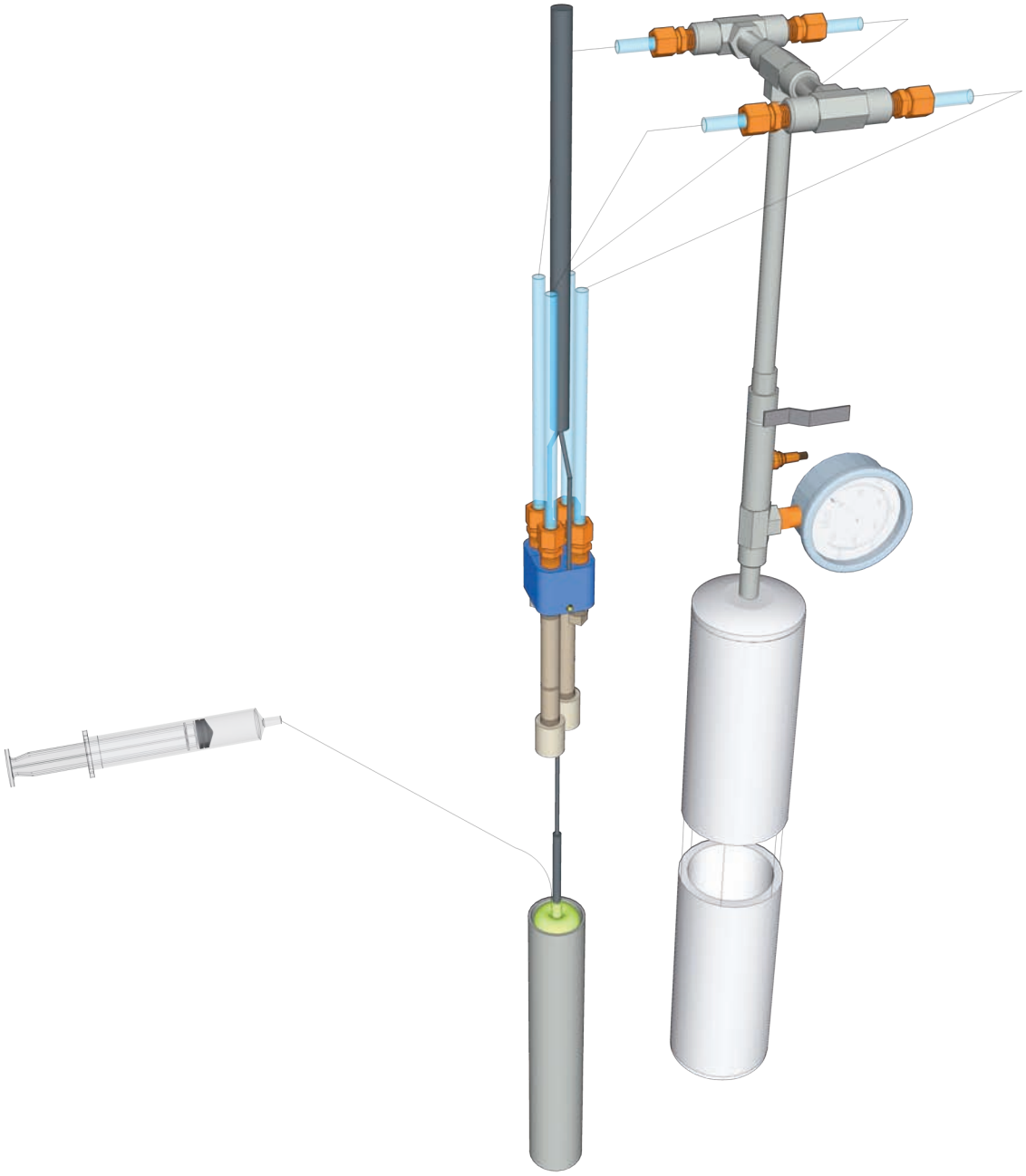

FIGURE A.21: Prototype 6d

A.10 Prototype 7a

A.10.1 Description

Prototype 7a (see Figure A.22) is a 3-foot long 1/8” stainless steel pipe that ends in a threaded T-connection. A ball joint connection is threaded into the bottom of the

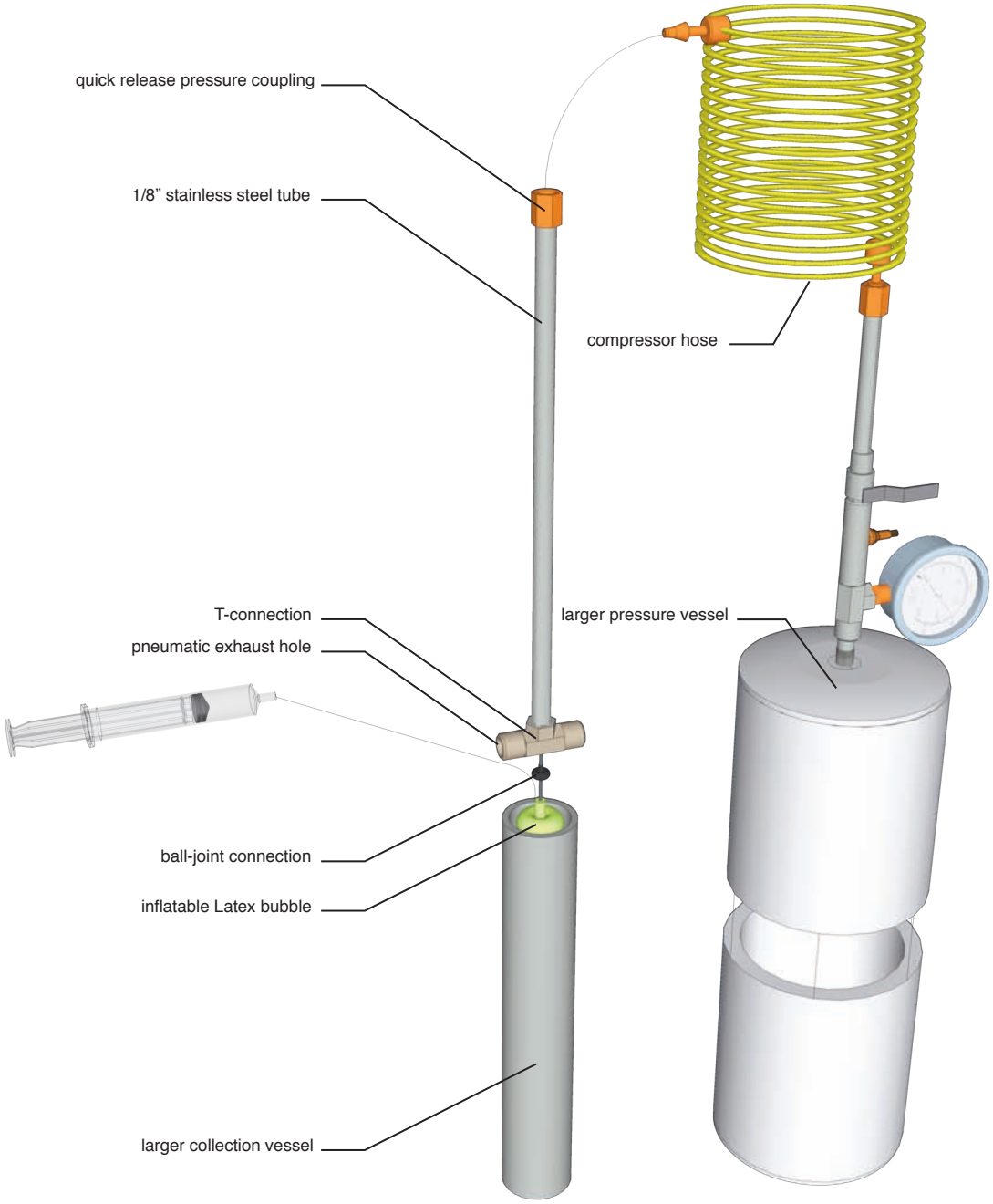

FIGURE A.22: Prototype 7a

T-connection and attaches to the catchment tube below. The catchment tube is adjusted to be nearly the diameter of the test hole. The pressure cell is enlarged to a 4” diameter by 4-foot long PVC pipe in the same configuration as the previous pressure cell. The tube connecting the pressure cell to the prototype is a 1/4” air compressor hose (10-foot long coil hose with a quick release).

A.10.2 Design Analysis

- Test yield decreased significantly. The two openings of the 1/8” T-connection were less effective at dislodging sand from the walls of the test hole.
- The larger pressure cell generated a longer release of pressurized air but not necessarily a stronger release of pressure.
- Disturbed test sand still had a tendency to sit on and around the threaded T-connection.
- The larger catchment tube functioned properly and collected more sand than the previous model would have.

A.10.3 Projected Adjustments

- A larger diameter air hose will be used between the pressure cell and the prototype to increase air flow and, therefore, the intensity of the air stream leaving the prototype.
- The openings of the T-connection should be reduced to create a more directed air stream leaving the prototype.

A.11 Prototype 7b

A.11.1 Description

Prototype 7b (see Figure A.23) is Prototype 7a with a larger connection hose (1/4” hose enlarged to 1/2”) connecting the pressure cell to the prototype. 1/8” threaded plugs are placed in the openings of the T-connection and center-drilled with an 1/8” bit (note: the inside diameter of the 1/8” NPT T-connection is .269” before being plugged and drilled to .125”).

A.11.2 Design Analysis

- The larger connection hose increased the intensity of the air stream significantly.

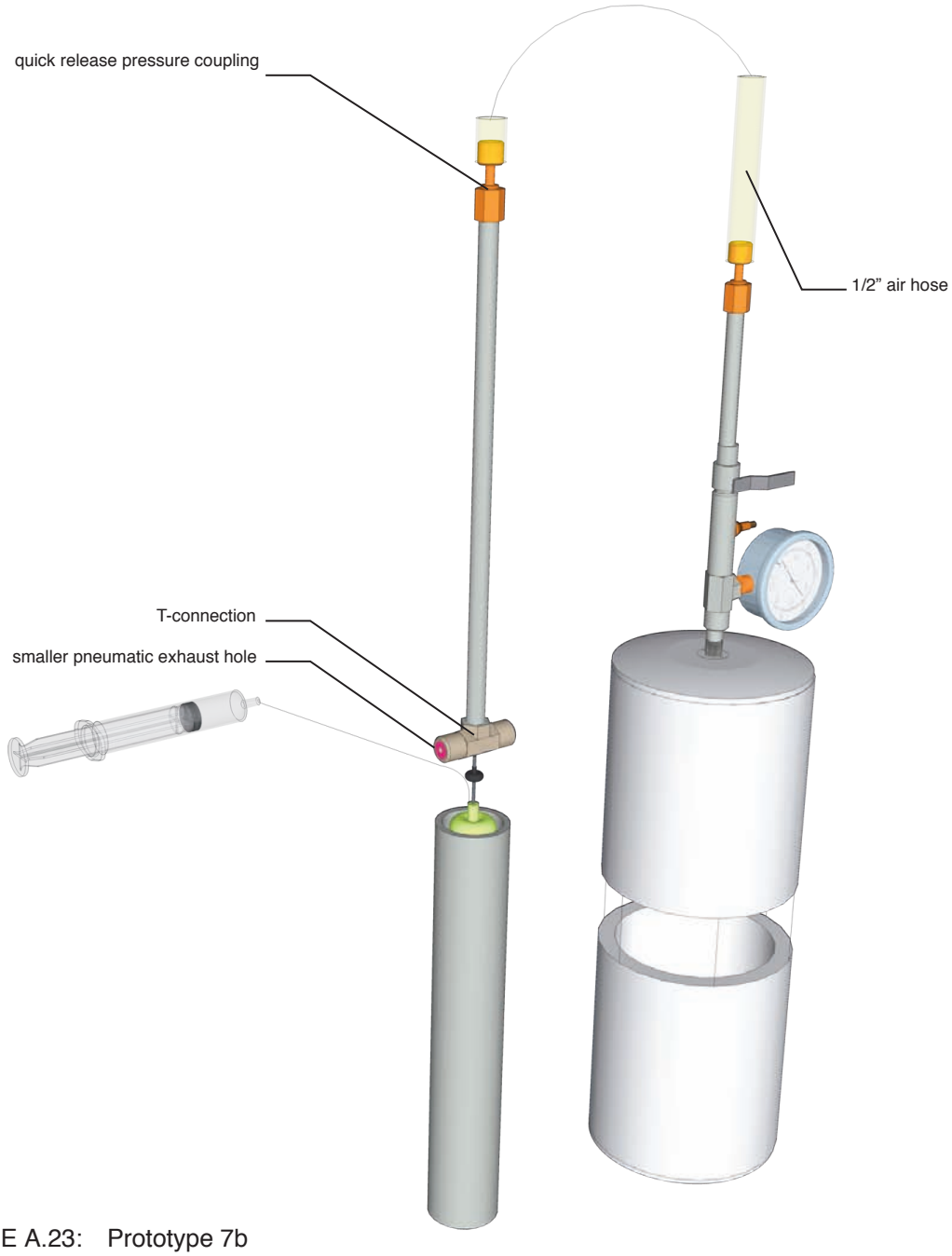

FIGURE A.23: Prototype 7b

- Test yields increased but were still too small to justify the time required for extensive laboratory testing.
- The shape of the affected regions of the hole wall were very deep and narrow when compared to the slit configurations (see Figure A.24). This shape suggests that the air stream is boring out test sand rather than creating an instability in the hole wall that could

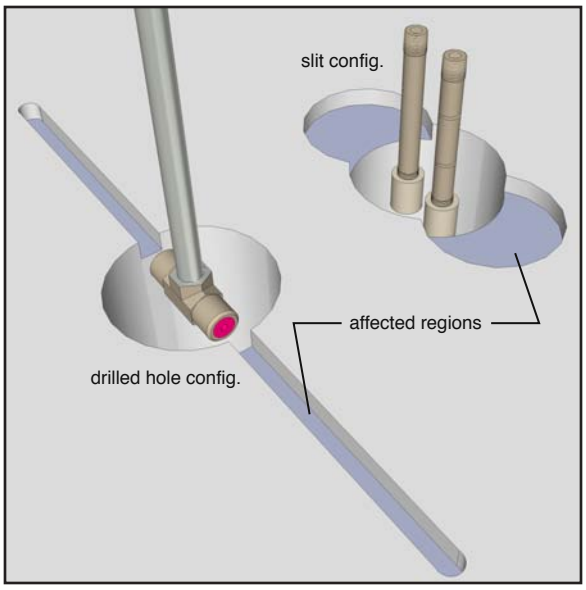

FIGURE A.24: Shape of Affected Regions

lead to a larger failure.

- The failed sand was still getting lodged on and around the prototype.

A.11.3 Projected Adjustments

•The pneumatic nozzle configuration should revert back to slits rather than drilled holes

•The threaded T-connection should be replaced with a straight pipe in order to reduce the area on which disturbed test sample can settle.

A.12 Prototype 8

A.12.1 Description

Prototype 8 (see Figure A.25) is Prototype 7b with the threaded T-connection is replaced by a 3-inch long 1/8" pipe. Two slits are cut on opposing sides of the pipe through which the pressurized air is distributed.

A.12.2 Design Analysis

- The design collected far more test sample than any prototype to date.
- Although the amount of sand becoming lodged on and around the prototype during testing has been greatly reduced, it was still a source of test variation that should be addressed.
- The performance of this prototype was very close to meriting extensive laboratory trials.

A.12.3 Projected Adjustments

- A prototype will be developed that will control the flow of the expelled air to capture the test sand that was becoming lodged on and around the pneumatic triggering nozzle.

• A conical tip will be added to the catchment tube to assist in advancing the prototype into the test hole even if the hole has squeezed inward after the dummy cone is removed.

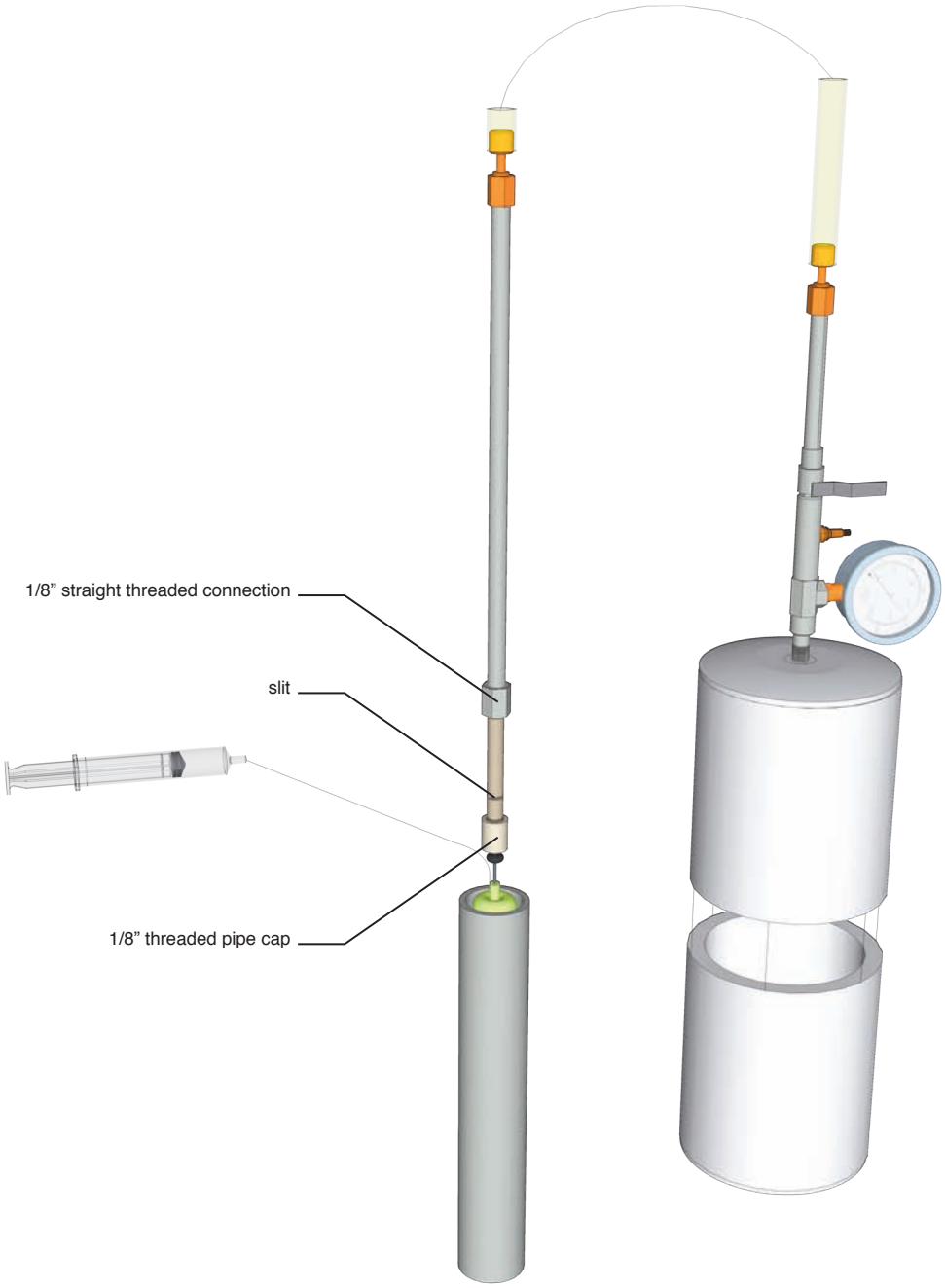

FIGURE A.25: Prototype 8

A.13 Prototype 9 (PISCIS)

A.13.1 Description

Prototype 9 (see Figure A.26) uses the same pneumatic triggering nozzle, pressure cell, and air tubing as Prototype 8 but has a newly designed catchment system and ventilation lid. The catchment tube is 1.69" in diameter and has a truncated 60º conical tip. The lid is also 1.69" in diameter and has a truncated 60º conical top to assist in removing the device from the test hole. The lid fits tightly with the catchment tube to be able to completely seal the PISCIS as it is placed in the test hole and after the test is run to preserve sample integrity and guarantee test repeatability. The PISCIS is advanced into the test hole in the closed position, where it is then opened by pulling up on two of the ventilation tubes that extend to the surface. The air is then released from the pressure cell and the lid is then returned to the closed position before the PISCIS is removed from the test hole.

A.13.2 Design Analysis

- The design yielded more collected sample than any prototype to date and did so with far less variation and excellent repeatability.
- The design allowed the pneumatic distribution nozzle to be easily removed, adjusted, and replaced if needed.
- Nylon mesh was used to cap each ventilation tube to keep any dislodged test sand from leaving the PISCIS with the expelled air, which further increased the repeatability of the test procedure.

A.13.3 Projected Adjustments

- Minor design adjustments could be executed to make the retrieval of the collected sample from within the PISCIS easier. Consider a threaded bottom cone to access the sample without having to invert the collection vessel.
- The filtration of exhaust air should take place within the lid before it reaches the ventilation tubes to prevent sample from clogging the tubes.
- Other design considerations must be evaluated if the PISCIS is to be commercialized (materiality, machine-ability, durability, cleaning process, replacement parts, etc.).

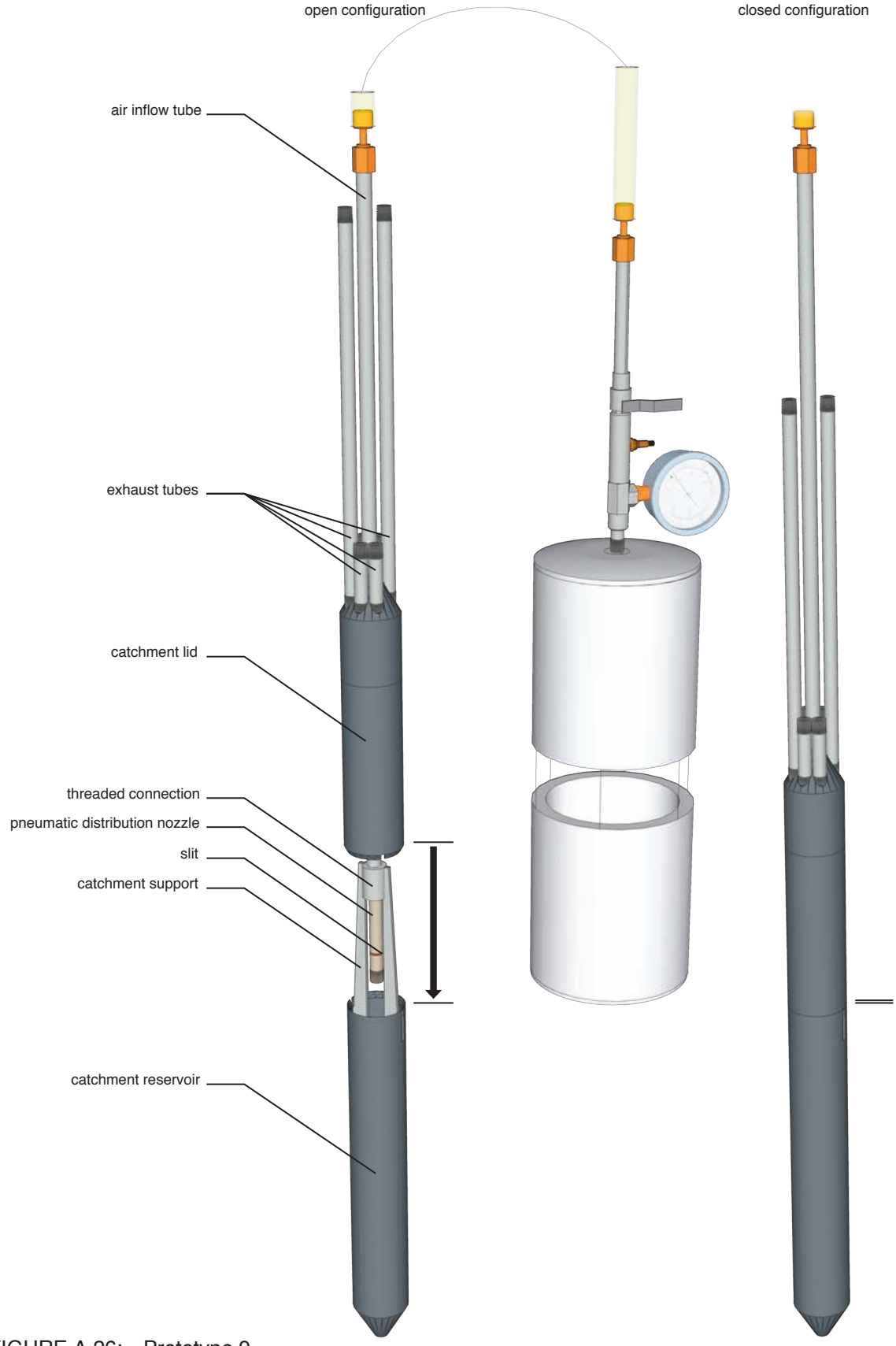

FIGURE A.26: Prototype 9